haematologica
Journal of the Ferrata Storti Foundation

A novel CCL3-HMGB1 signaling axis regulating osteocyte RANKL expression in multiple myeloma

by Aric Anloague, Hayley M. Sabol, Japneet Kaur, Sharmin Khan, Cody Ashby, Carolina Schinke, C. Lowry Barnes, Farah Alturkmani, Elena Ambrogini, Michael Tveden Gundesen, Thomas Lund, Anne Kristine Amstrup, Thomas Levin Andersen, Marta Diaz-delCastillo, G. David Roodman, Teresita Bellido, and Jesus Delgado-Calle

Received: August 20, 2024.
Accepted: November 15, 2024.

Citation: Aric Anloague, Hayley M. Sabol, Japneet Kaur, Sharmin Khan, Cody Ashby, Carolina Schinke, C. Lowry Barnes, Farah Alturkmani, Elena Ambrogini, Michael Tveden Gundesen, Thomas Lund, Anne Kristine Amstrup, Thomas Levin Andersen, Marta Diaz-delCastillo, G. David Roodman, Teresita Bellido, and Jesus Delgado-Calle.
A novel CCL3-HMGB1 signaling axis regulating osteocyte RANKL expression in multiple myeloma. Haematologica. 2024 Nov 28. doi: 10.3324/haematol.2024.286484 [Epub ahead of print]

A novel CCL3-HMGB1 signaling axis regulating osteocyte RANKL expression in multiple myeloma

Aric Anloague[1], Hayley M. Sabol[1], Japneet Kaur[1,2], Sharmin Khan[1], Cody Ashby[2,3], Carolina Schinke[2,4], C. Lowry Barnes[5], Farah Alturkmani[6,7], Elena Ambrogini[6,7,8], Michael Tveden Gundesen[9,10], Thomas Lund[9,10,11], Anne Kristine Amstrup[12], Thomas Levin Andersen[10,13,14], Marta Diaz-delCastillo[9], G. David Roodman[15], Teresita Bellido[1,2,5,7,8], and Jesus Delgado-Calle[1,2,5,7*]

[1]Physiology and Cell Biology, University of Arkansas for Medical Sciences, Little Rock, AR, US; [2]Winthrop P. Rockefeller Cancer Institute, University of Arkansas for Medical Sciences, Little Rock, US; [3]Department of Biomedical Informatics, University of Arkansas for Medical Sciences, Little Rock, AR, US; [4]Myeloma Center, University of Arkansas for Medical Sciences, Little Rock, AR, US; [5]Department of Orthopedic Surgery; University of Arkansas for Medical Sciences, Little Rock, AR, US; [6]Division of Endocrinology and Metabolism, University of Arkansas for Medical Sciences and Central Arkansas Veterans Healthcare System, Little Rock, AR, US; [7]Center for Musculoskeletal Disease Research, University of Arkansas for Medical Sciences Little Rock, AR, US; [8]Central Arkansas Veterans Healthcare System, Little Rock, AR, US; [9]Department of Hematology, Odense University Hospital, Odense, Denmark; [10]Department of Clinical Research, University of Southern Denmark, Odense, Denmark; [11]Centre for Innovative Medical Technology, Odense University Hospital, Odense, Denmark; [12]Department of Endocrinology and Internal Medicine (MEA), THG, Aarhus University Hospital, Aarhus, Denmark; [13]Department of Pathology, Odense University Hospital, Odense, Denmark;

[14]Department of Forensic Medicine, University of Aarhus, Aarhus, Denmark; [15]Division of Hematology and Oncology, Department of Medicine, Indiana University, Indianapolis, IN, US.

Author contributions

J.D.C., T.B., and G.D.R. conceived the project. J.D.C. supervised the study. A.A., H.M.S., J.K., C.A., C.S., T.B., G.D.R., and J.D.C. designed the experiments. A.A., H.M.S., J.K., C.A., C.S., S.K., C.L.B., F.A., E.A., M.T.G., T.L., A.K.A., T.L.A., and M.D.C., performed the experiments and/or collected data. A.A., C.S., C.A., and J.D.C. contributed to the data analysis and interpretation. J.D.C and A.A. wrote the manuscript. All authors reviewed the manuscript.

Running head: Osteocytic RANKL in multiple myeloma

Keywords: multiple myeloma, osteocytes, RANKL, bone, osteoclasts, resorption

***Corresponding author:** Jesús Delgado-Calle, Ph.D., Department of Physiology and Cell Biology, University of Arkansas for Medical Sciences, 4301 W. Markham St. Little Rock, AR 7220,5, E-mail: jdelgadocalle@uams.edu, Office: +1-501-686-7668; ORCID: 0000-0002-2083-2774.

Data sharing statement. The IA15 datasets used for the analyses described in this work were downloaded from the Multiple Myeloma Research Foundation CoMMpass (MMRF CoMMpass [SM] (Relating Clinical Outcomes in MM to Personal Assessment of Genetic Profile) study (www.themmrf.org)) researcher gateway. Other non-public datasets used and analyzed during the current study are available from the corresponding author upon reasonable request.

Acknowledgments: The authors would like to acknowledge the services provided by the TBAPS of the UAMS Winthrop P. Rockefeller Cancer Institute, Dr. Manish Adhikari and Kaja S. Laursen for assistance with histological tissue processing, and the MMRF for providing the CoMMpass IA15 dataset. These data were generated as part of the Multiple Myeloma Research Foundation Personalized Medicine Initiatives (https://research.themmrf.org and www.themmrf.org).

Funding: This work was supported by the National Institutes of Health (NIH) R01CA209882 (J.D.C. and T.B.), R37CA251763 (J.D.C.), R01CA241677 (J.D.C.), P20GM125503 (J.D.C and E.A.), F31CA284655 (H.M.S.), a KL2 TR003108 grant through the National Center for Advancing Translational Sciences of the NIH (C.A.), AG075227 to M.D.C and T.L.A., and the UAMS Winthrop P. Rockefeller Cancer Institute Seeds of Science Award and Voucher Program (J.D.C.), and the Veterans Administration I01 BX002104 and IK6BX004596 awards (T.B.).

Disclosure of Conflicts of Interest: The authors have declared that no conflict of interest exists.

Abstract

Multiple myeloma (MM) is a clonal plasma cell proliferative malignancy characterized by a debilitating bone disease. Osteolytic destruction, a hallmark of MM, is driven by increased osteoclast number and exacerbated bone resorption, primarily fueled by the excessive production of RANKL, the master regulator of osteoclast formation, within the tumor niche. We previously reported that osteocytes, the most abundant cells in the bone niche, promote tumor progression and support MM bone disease by overproducing RANKL. However, the molecular mechanisms underlying RANKL dysregulation in osteocytes in the context of MM bone disease are not entirely understood. Here, we present evidence that MM-derived CCL3 induces upregulation of RANKL expression in both human and murine osteocytes. Through a combination of *in vitro, ex vivo*, and *in vivo* models and clinical data, we demonstrate that genetic or pharmacologic inhibition of CCL3 prevents RANKL upregulation in osteocytes and attenuates the bone loss induced by MM cells. Mechanistic studies revealed that MM-derived CCL3 triggers the secretion of HMGB1 by osteocytes, a process required for osteocytic RANKL upregulation by MM cells. These findings identify a previously unknown CCL3-HMGB1 signaling axis in the MM tumor niche that drives bone resorption by promoting RANKL overproduction in osteocytes.

Introduction

Multiple myeloma (MM) is a hematological malignancy characterized by the proliferation of malignant plasma cells within the bone marrow, resulting in a devastating bone disease in the majority of patients.[1] More than 80% of patients diagnosed with MM present bone lesions and experience skeletal-related events, including pathologic fractures or spinal cord compression, which increase mortality and morbidity and severely decrease their quality of life.[2, 3] Despite the tremendous therapeutic advances made in the last decade in improving survival in MM patients, patients often relapse, causing further bone destruction. Thus, improving bone health remains an unmet medical need in MM.

The bone disease stems from tumor-induced osteoclastogenesis and osteoblast suppression, thereby creating a self-sustained cycle of bone destruction and tumor progression.[4] Central to MM skeletal pathology is the dysregulation of the *Receptor activator of nuclear factor-kappa B ligand* (*TNFSF11*; referred to in this paper as *RANKL*), a key mediator of osteoclast differentiation and function.[5, 6] The aberrant overexpression of *RANKL* by MM cells and cells of the tumor niche, coupled with the suppression of *Osteoprotegerin* (*TNFRSF11B*; referred to in this paper as *OPG*),[5] tips the balance of bone homeostasis towards unchecked osteoclastogenesis and bone resorption. Thus, understanding the cellular sources and molecular mechanisms driving RANKL dysregulation in MM is imperative to restore physiological bone homeostasis and find new targets to treat MM bone disease.

Osteocytes are terminally differentiated osteoblasts embedded in the mineral matrix, make up the majority of all bone cells, are a source of RANKL in bone, and serve as crucial regulators of osteoclastogenesis under physiological conditions.[7, 8] Recent insights have highlighted that osteocytes respond to pathological cues in MM and contribute to MM progression and the

associated bone disease.[9-13] In the context of MM bone disease, osteocytes respond to tumor-derived signals by undergoing apoptosis and overproducing RANKL to attract osteoclast precursors, further amplifying osteoclast formation and promoting local bone destruction.[5] However, the mechanisms mediating the communication between MM and osteocytes are not entirely understood. In this study, we identify *Macrophage inflammatory protein 1 alpha* (*CCL3*) as a significant mediator of the crosstalk between MM cells and osteocytes and describe a novel signaling axis meditating osteocytic RANKL dysregulation initiated by MM-derived CCL3 and executed by autocrine *High mobility group box 1* (HMBG1) signaling in osteocytes.

Methods

Study population. We obtained MM patient gene expression and clinical data from the Multiple Myeloma Research Foundation (MMRF) CoMMpass registry (NCT01454297, version IA13). From an initial 921 patients with accessible gene expression data in the CoMMpass registry, 757 samples at diagnosis (NDMM) were selected, as shown before.[12] Salmon gene count data were imported into and normalized using the R package DESeq2. To determine patients with high versus low *CCL3* expression, we compared the top vs. bottom quartiles.[12]

Cell Culture. Human JJN3 MM cells (RRID:CVCL_2078) were obtained from N. Giuliani (University of Parma, Italy). Murine 5TGM1 MM cells (RRID: CVCL_VI66) were obtained from Dr. B. Oyajobi (University of Texas at San Antonio, TX, USA). All MM cells were cultured in RPMI with 10% FBS, 1% penicillin and streptomycin, 0.2% Normocin, and 0.1% plasmocin. Murine Ocy454 (RRID:CVCL_UW31) osteocyte-like cells were provided by Dr. Pajevic (Boston University, MA, US) and were maintained in alpha-MEM media with 10% FBS, 1% penicillin and streptomycin, 0.2% Normocin, and 0.1% plasmocin. MLO-A5 (RRID: 19

CVCL_0P24) and MLOY4 (RRID:CVCL_M098) murine osteocyte-like cells were purchased from Kerafast (Boston, MA, USA). MLOA5 and MLOY4 cells were cultured on calf skin collagen type I-coated plates using alpha-MEM media with 2.5% FBS, 2.5% BCS, 1% penicillin and streptomycin, 0.2% Normocin, and 0.1% plasmocin. Cell lines were checked for mycoplasma weekly and routinely examined for proper morphology, population doubling, and paraprotein production. Conditioned media (CM) from JJN3/5TGM1 $2x10^6$ MM cells was collected after 48h of culture. Osteocyte-like cell lines were cultured with/without 50% CM, as described before,[5, 12] in the presence/absence of an anti-HMGB1 neutralizing antibody (10ug/mL), recombinant CCL3 (1ug/mL), or an anti-CCL3 neutralizing antibody (0.05ug/mL) for 24-48h. Reagents are described in **Supplementary Methods**.

Genetic inhibition in MM cells and osteocyte-like cells. Methods used to manipulate *CCL3/HMGB1* expression are described in **Supplementary Methods**.

Cell death and proliferation assays. Proliferation and cell death in MM cells were assessed by Trypan Blue exclusion, as reported before.[5, 12]

Animal studies. 7-week-old immunocompetent C57BL/KaLwRijHsd mice were injected intravenously with $1x10^6$ 5TGM1 MM cells or saline and sacrificed after 4 weeks. 7-week-old immunodeficient NSG mice were injected intravenously with $1x10^6$ JJN3 cells and sacrificed after 4 weeks. 7-week-old NSG mice were intratibially injected with saline, $1x10^5$ JJN3 control (Ctl) or JJN3- $CCL3^{KD}$ cells in both tibias and sacrificed after 4 weeks. The sample size was calculated based on previous studies.[5, 12] The levels of the tumor biomarker Human Kappa light chain (Bethyl Laboratories, Cat. #NC0102649) were used to determine tumor growth/burden *in vivo* (serum) and *ex vivo* (conditioned media). Bone mass and microarchitecture were assessed using microCT, as shown before.[5, 12]

***Ex vivo* Bone Organ Cultures.** *Ex vivo* MM-murine bone organ cultures were established as described before.[5] Ex vivo MM-human bone organ cultures were established with human cancellous bone fragments similar in size obtained from femoral heads discarded after hip arthroplasty (see **Supplementary Methods** for details).

Gene expression. Methods to quantify mRNA (qPCR) and protein expression (Western Blot and ELISA) are described in **Supplementary Methods**.

RNA in-situ hybridization (RNAscope). RNA in situ hybridization was performed using the RNAScope 2.5 HD detection reagent RED kit from Advanced Cell Diagnostics (Newark, CA, US) following the manufacturer's instructions, as previously described.[14] The following probes were incubated on paraffin-embedded tissue sections for 2 hours at 40C: murine *Rankl* (Cat #410921) and positive/negative controls (Cat #313911, Cat #310043). The signal was then detected at room temperature for 10 min. Sections were counterstained with hematoxylin, dehydrated at 60C for 20 min, and mounted using VectaMount permanent mounting medium (Vector Laboratories, Newark, CA, US). The number of positive and negative osteocytes was quantified using a brightfield microscope at 40X magnification. Analyses were performed in the cortical bone of an 800-μm region of the tibia, starting 200 μm below the growth plate, in a blinded fashion by two independent investigators.

Human samples methods and histological analysis. Methods to quantify *RANKL* mRNA and HMGB1 protein expression in histological sections from healthy subjects (n=5) and newly diagnosed MM patients (n=6) are described in **Supplementary Methods**.

Statistics. Data were analyzed using GraphPad (GraphPad Software Inc, San Diego, CA, USA). Differences in means were analyzed using a combination of unpaired *t*-test and One-Way ANOVA tests, followed by pairwise multiple comparisons (Tukey post hoc test). Values were

reported as means ± SD, unless otherwise indicated in the figure legends. P values ≤ 0.05 were considered statistically significant. Data analysis was performed in a blinded fashion.

Study Approvals. All procedures involving animals were performed in accordance with guidelines issued by the University of Arkansas for Medical Sciences IACUC (protocol #2022200000489). Collection and de-identification of human bone samples were coordinated by the UAMS Winthrop P. Rockefeller Cancer Institute TBAPS and approved by the UAMS IRB (protocol #262940). All participants provided written, informed consent before study procedures occurred, with continuous consent ensured throughout participation. Trephine iliac crest bone marrow biopsies from patients with newly diagnosed MM (mean age ± standard deviation 72.17 ± 10.74 years old) were retrieved from Danish histopathological biobanks under approval from the Danish National Committee on Biomedical Research Ethics (S-20190110); biopsies from control individuals (ages 68.18 ± 4.27 years old) were collected under approval from the Regional Committee (1-10-72-223-20) and upon collection of written consent. All human samples were collected and processed in accordance with the Declaration of Helsinki.

Results

MM cells produce soluble factors that upregulate RANKL expression in osteocytes. We previously reported that upon intratibial injections of JJN3 MM cells, the prevalence of osteocytes expressing RANKL increases and that CM from JJN3 MM cells increases *Rankl* expression in early osteocytes.[5] Here, we expanded on our initial observations and report that intravenous injection of human JJN3 (**Figure 1A**) or murine 5TGM1 (**Figure 1B**) MM cells and the subsequent infiltration and growth of MM cells in bone also increases the expression of *Rankl* in bone. Moreover, we found that treatment with human or murine MM-CM upregulated

Rankl expression in Ocy454 (mature osteocytes), MLO-Y4 (mature osteocytes), and MLO-A5 (early osteocytes) (**Figures 1C** and **D**). We also detected decreases in the expression of *Opg*, a soluble decoy receptor for RANKL,[15] and a higher *Rankl/Opg* ratio in bones infiltrated with MM cells and osteocytes exposed to factors derived from MM cells (**Suppl. Figure 1**). Together, these *in vivo* and *in vitro* findings show that cytokines derived from MM cells reprogram RANKL skeletal expression and raise the possibility that also mediated RANKL upregulation in osteocytes.

MM-derived CCL3 increases RANKL expression and secretion in osteocytes. MM cells secrete a wide variety of cytokines that reprogram cells of the tumor niche and are critical in the induction of osteolysis. Here, we focused on CCL3, a pro-inflammatory chemokine highly secreted by MM cells in MM patients compared to healthy subjects and linked to bone resorption and MM bone disease.[16-23] We found that CCL3 expression in $CD138^+$ cells is associated with poor prognosis in newly diagnosed MM (NDMM) patients (**Figures 2A** and **B**). We next investigated its role as a potential regulator of osteocytic RANKL in the context of MM. We detected human *CCL3* mRNA expression in bones infiltrated with human JJN3 MM cells (**Figure 2C**). In contrast, murine *Ccl3* mRNA expression coming from the microenvironment was not affected by MM cells (**Figure 2C**), suggesting MM cells are the primary source of this chemokine in the MM tumor niche. We also observed a 3-fold increase in murine *Ccl3* mRNA expression in bones bearing murine 5TGM1 MM cells (**Figure 2D**). Consistent with the potential role of this chemokine in the regulation of osteocytic RANKL, we detected the expression of the CCL3 receptors C-C motif chemokine receptor (*Ccr) 1*, *3*, and *5*, in osteocyte-like cells, being *Ccr5* the most highly expressed receptor (**Figure 2E**).

To determine the impact of CCL3 on RANKL expression in osteocytes, we used a combination of *in vitro* and *ex vivo* approaches. We found that treatment with recombinant (r) CCL3 upregulated *Rankl* mRNA and protein levels (**Figure 3A** and **C**), had minor effects on *Opg* mRNA expression, and increased the *Rankl/Opg* ratio (**Suppl. Figure 2**) in osteocyte-like cells. Treatment with rCCL3 also increased *Rankl* expression in murine bones cultured *ex vivo* containing authentic osteocytes (**Figure 3B**). To investigate the role of MM-derived CCL3, we stably knocked it down ($CCL3^{KD}$) in JJN3 MM cells (**Suppl. Figure 3A)**. CM from control (Ctl) MM cells increased by 4-fold RANKL protein production (cell lysates) and secretion (CM) by Ocy-454 cells (**Figure 3C**). While $CCL3^{KD}$ cells also stimulated RANKL secretion in Ocy-454, this effect was reduced by 50% compared to Ctl MM cells (**Figure 3C**). Similarly, transient inhibition of *CCL3* in MM cells with siRNAs prevented the upregulation of *Rankl* in MLO-A5 osteocyte-like cells (**Suppl. Figure 3B-C).** Next, we used a neutralizing antibody to block MM-derived CCL3 signaling pharmacologically. The *Rankl* upregulation seen in osteocyte-like cells treated with CM from JJN3 or 5TGM1 MM cells was blocked by the anti-CCL3 neutralizing antibody (**Figure 3D** and **E**). Collectively, these results suggested a causal role of MM-derived CCL3 signaling on RANKL overproduction by osteocytes.

Genetic deletion of *CCL3* in MM cells decreases tumor growth, bone destruction, and RANKL in osteocytes. Next, we assessed *in vivo* the impact of MM-derived CCL3 on *Rankl* expression in osteocytes and bone mass. Immunodeficient mice were injected intratibially with saline, Ctl, or $CCL3^{KD}$ JJN3 MM cells. $CCL3^{KD}$ cells retained a 90% reduction in *CCL3* expression compared to Ctl MM cells for 4 weeks (**Figure 4A**). Mice bearing Ctl MM cells had exponential tumor growth and a 70% decrease in tibial cancellous bone mass compared to naïve mice (**Figures 4B-E**). $CCL3^{KD}$ MM cells did not exhibit changes in proliferation/viability vs. Ctl

MM cells *in vitro* (**Suppl. Figure 4A and B**). However, mice injected with *CCL3*^{KD} MM cells showed a 90% reduction in tumor growth and higher bone volume (50% more) compared to mice injected with Ctl MM cells (**Figures 4B-E**).

The dramatic bone loss seen with Ctl MM cells was accompanied by a 4-fold increase in the number of cortical osteocytes expressing *Rankl*, assessed by mRNA *in situ* hybridization (**Figure 5A**). The number of osteocytes expressing mRNA *Rankl* was reduced by 50% in bones bearing *CCL3*^{KD} cells compared to mice injected with Ctl MM cells (**Figure 5A**). Prompted by this *in situ* observation, we explored further the impact of MM-derived CCL3 in the regulation of *RANKL* in *ex vivo* 3D organ cultures established with human bones containing human osteocytes. As seen in the mouse studies, we detected active tumor growth and higher expression of *RANKL* and *CCL3* in human bones infiltrated with Ctl MM cells cultured *ex vivo* **(Figure 5B)**. In contrast, tumor growth was reduced by 60%, and *RANKL* and *CCL3* expression remained unchanged in bones infiltrated by *CCL3*^{KD} MM cells **(Figure 5B)**. To circumvent the potential confounding effect of the differential tumor burden on the contribution of MM-derived CCL3 to *RANKL* upregulation in osteocytes, we treated human bones with CM collected from the same number of Ctl and *CCL3*^{KD} MM cells. CM from Ctl MM cells increased *RANKL* expression, whereas CM from *CCL3*^{KD} MM cells did not affect *RANKL* expression in human bones cultured *ex vivo* (**Figure 5C**). Both infiltration of Ctl MM cells or treatment with CM from Ctl MM cells decreased *OPG* expression in human bones cultured *ex vivo*, and this effect was not seen with *CCL3*^{KD} MM cells or their CM (**Figures 5B** and **C**). Of note, we observed *in vitro* that *CCL3*^{KD} MM cells exhibited a modest reduction in *RANKL* mRNA expression, with no changes in *OPG* (**Suppl. Figure 4C**).

HMGB1 released by osteocytes mediates CCL3-induced RANKL upregulation. We previously reported that MM cells induced osteocyte apoptosis, a phenomenon that partially contributed to osteocyte *Rankl* upregulation.[5] HMGB1 is a pro-inflammatory cytokine ("alarmin") released by dying cells, including osteocytes.[24] Extracellular HMGB1 has been shown to stimulate RANKL *in vitro* in stromal cells and osteocytes.[24, 25] We found that *Hmgb1* expression at the mRNA level was not affected in bones bearing MM tumors (**Figure 6A** and **B**), osteocyte-like cells treated with CM from MM cells or rCCL3, or bones treated with CM from JJN3 cells cultured *ex vivo* (**Suppl. Figure 5A-D**). We next investigated if HMGB1 release by osteocytes is affected by MM cells. CM from Ctl JJN3 MM cells increased by 2-fold the secretion of HMGB1 and decreased the cellular levels in osteocyte-like cells (**Figure 6C** and **D; Suppl. Figure 5E** and **F**). In contrast, osteocytes did not affect HMGB1 levels in JJN3 MM cells (**Suppl. Figure 5F**). The extracellular release of HMGB1 was not detected when osteocytes were cultured with CM from *CCL3*^{KD} cells, and it was prevented by treatment with an anti-CCL3 neutralizing antibody (**Figure 6C** and **D**). Remarkably, recombinant CCL3 did not induce osteocyte cell death, and pharmacologic or genetic inhibition of CCL3 did not affect MM-induced osteocytic cell death (**Suppl. Figure 6A**), suggesting CCL3 signaling triggers HMGB1 secretion in osteocytes independently of cell death.

Thus, we next examined if HMGB1 contributes to osteocytic RANKL upregulation induced by MM-derived CCL3. Pharmacological blockade of HMGB1 with a neutralizing antibody (**Figure 7A** and **B**) or genetic knockdown of *Hmgb1* in osteocytes (**Figure 7C** and **Suppl. Figure 6B-D**) prevented the increases in *Rankl* mRNA expression and protein secretion (**Figure 7D**) in osteocytes cultured with CM from MM cells. Similarly, treatment with an anti-HMGB1 neutralizing antibody blocked the *Rankl* upregulation induced by rCCL3 (**Figure 7E**).

Lastly, we compared *RANKL* mRNA and HMGB1 protein expression in osteocytes in bone biopsies from a small cohort of healthy subjects and newly diagnosed MM patients. We detected a higher prevalence of *RANKL*$^{+}$, HMGB1^{+}, and double *RANKL*$^{+}$-HMGB1^{+} osteocytes in MM patients compared to healthy subjects (**Figure 8**). Together, these findings support the existence of a CCL3-HMGB1 signaling axis regulating osteocytic RANKL in the MM tumor niche.

Discussion

Bone disease in MM poses significant clinical challenges primarily due to its negative impact on patient quality of life, morbidity, and mortality.[2, 3, 26] While various cytokines released by MM cells or the tumor niche contribute to MM-induced bone destruction, RANKL signaling plays a central role in activating osteoclasts and driving bone resorption.[27] Osteocytes, which constitute a significant source of RANKL in adult bone, are reprogrammed by MM cells to overproduce RANKL and support bone destruction.[5] Yet, the molecular mechanisms underlying RANKL dysregulation in osteocytes in MM are not entirely understood. In this study, we discovered a new signaling axis regulating osteocytic RANKL production.[7, 8] We show that paracrine actions of MM-derived CCL3 on osteocytes trigger the secretion of HMGB1, which in an autocrine manner stimulates RANKL production in osteocytes. Further, we provide evidence that this signaling axis exists in MM patients and demonstrate that targeting CCL3 or HMGB1, either genetically or pharmacologically, decreases RANKL in osteocytes. Our data collectively identifies MM-derived CCL3 as a reprogramming signal for osteocytes, shifting their biological function to favor osteoclastogenesis and bone destruction in the MM tumor niche.

Previous research established that MM cells secrete CCL3 to promote osteoclastogenesis and bone resorption by acting directly on osteoclast progenitors through CCR1 or CCR5 or

enhancing the osteoclastogenic effects of RANKL.[16, 28-30] However, the role of CCL3 in regulating RANKL production within the tumor microenvironment has remained ambiguous, with conflicting *in vitro* results reported.[31, 32] Our study extends beyond *in vitro* cell culture systems to include *in vivo* mouse models of MM, *ex vivo* organ cultures established with human bone, and *in situ* hybridization in bone biopsies from MM patients. We found that osteocytes express *CCR1*, *CCR3,* and *CCR5* receptors and respond to CCL3 signals by producing RANKL. Collectively, these findings provide robust evidence that MM-derived CCL3 functions as a mediator for MM-osteocyte crosstalk and acts as an important regulator of RANKL in the MM tumor niche.

We and others reported before that MM cells induce osteocyte apoptosis *in vitro*, *in vivo*, and in MM patients. This increase in osteocyte apoptosis contributes to the upregulation of RANKL and the recruitment and activation of osteoclasts.[5, 33, 34] During osteocyte apoptosis, HMGB1 is released into the extracellular space through a passive process.[35] High serum HMGB1 levels are found in MM patients and are associated with disease progression.[36, 37] However, the mechanisms leading to HMGB1 over secretion in MM are unclear. Our research reveals that, in the context of MM, CCL3 signaling is a potent driver of HMGB1 release by osteocytes, independent of apoptosis. Our data demonstrates that CCL3 induces osteocytes to release HMGB1 through a mechanism that does not involve transcriptional changes in HMBG1 but rather initiates a program for active HMGB1 secretion into the extracellular space. The active release of HMGB1 is regulated by various factors, including related ROS and redox signals, TNF, Notch, or posttranslational modifications.[38] Further investigation beyond the scope of this manuscript is needed to elucidate the molecular mechanisms involved in CCL3 stimulation of HMGB1 release by osteocytes. Our results also suggest that osteocyte-derived HMGB1,

triggered by CCL3, signals in neighboring osteocytes to promote RANKL upregulation and production. This notion is supported by our observation of an increased prevalence in double *RANKL*$^{+}$-HMGB1^{+} osteocytes in MM patients, and it is consistent with prior findings showing that extracellular HMGB1 binds to RAGE receptors in osteocytes and increases RANKL expression.[25] These results uncover a new regulatory mechanism for HMGB1 release in osteocytes and a novel CCL3-HMGB1 signaling axis regulating pathological RANKL expression in osteocytes.

Manipulation of CCL3 and HMGB1 effectively prevented the upregulation of RANKL in osteocytes induced by MM cells in *in vitro* culture systems. However, *in vivo* or *ex vivo* systems, which more accurately replicate the complexity of the bone tumor niche, showed only partial inhibition of RANKL dysregulation in osteocytes when these signals were inhibited. In addition to MM-derived CCL3, osteocyte apoptosis[5, 33, 34] and MM-secreted 2-deoxy-D-ribose, which upregulates CIITA expression in osteocytes,[39] have been postulated as potential mechanisms regulating RANKL in osteocytes by MM cells, which may account for the incomplete prevention of osteocytic RANKL expression in our studies. Similar to our current findings with CCL3, inhibition of apoptosis or CIITA also failed to fully prevent RANKL upregulation in osteocytes by MM cells.[5, 39] CCL3 from other cells of the tumor niche could also influence RANKL expression in osteocytes. Moreover, we only found partial prevention of bone loss in mice injected with *CCL3*-silenced MM cells, suggesting that other mechanisms independent of CCL3 and/or RANKL drive bone destruction in MM. Thus, RANKL and MM bone destruction are likely supported by various mechanisms that may function in a dynamic, context-dependent manner to ensure continuous bone resorption, thereby providing a constant source of growth factors from bone that support tumor growth and survival.

We also found that higher expression of CCL3 in $CD138^+$ cells is associated with poorer overall survival and progression-free survival in newly diagnosed MM patients. These findings are in line with prior clinical observations linking high serum levels of CCL3 with disease progression and adverse prognosis.[19-23] Consistent with its impact on disease progression, we found that genetic inhibition of CCL3 in MM cells severely impairs their growth *in vivo* in mice, as seen previously by others[30, 40], and *ex vivo* in human bones. However, the growth retardation was not observed when the MM cells were cultured alone *in vitro*. This discrepancy is attributed to the decreased expression of α5β1 integrin following CCL3 inhibition, which reduces the ability of MM cells to adhere to marrow stromal cells that support their growth.[29, 41] We also noted a reduction in RANKL expression in MM cells following CCL3 inhibition, suggesting that autocrine CCL3 signals not only regulate the expression of adherence molecules in MM cells but also their osteoclastogenic potential. Additionally, our data suggest that the CCL3 paracrine regulation of RANKL in osteocytes operates independently of its effects on tumor growth, as shown by our studies using the same number of control and CCL3 knockdown MM cells in *ex vivo* human bone models. However, because the autocrine and paracrine effects of CCL3 on RANKL on MM cells and osteocytes occur simultaneously and are interrelated in our mouse model, we were unable to distinctly separate their specific contribution to MM-induced bone loss, which we acknowledge as a limitation of the current study.

Anti-resorptive therapy effectively reduces fracture risk and bone pain in multiple MM patients. However, long-term use of bisphosphonates can excessively suppress bone resorption and remodeling, leading to side effects like jaw osteonecrosis and atypical fractures.[42, 43] Denosumab, an anti-RANKL antibody, offers a therapeutic alternative by blocking RANKL signaling,[44] preventing osteoclast formation, but also reducing osteoblasts. Denosumab and

bisphosphonates in MM patients exhibit a similar risk for jaw osteonecrosis.[44, 45] Further, when Denosumab is stopped, rapid increases in osteoclast activity and bone resorption can occur, elevating fracture risk. [14, 46] Our data and the current knowledge on CCL3 signaling suggest that targeting this molecule could reduce the pathological RANKL upregulation associated with MM to near-physiological levels, preserve bone mass, as well as potentially restore osteoblast function in MM.[18] This approach may offer a therapeutic advantage over current anti-resorptive therapies by reducing resorption without completely halting it, which may promote healthy bone remodeling. CCL3 has also been linked to other aspects of MM disease, including immune suppression, responses to therapy, and anemia, which such a therapy could also alleviate.[40, 47-52] Though targeting CCL3 signals has shown promising results in preclinical studies,[40, 47-52] the use of antibodies or small molecules (CCR1 antagonists) aimed at this pathway remains limited in the clinical setting.[48]

In summary, this study reveals that CCL3 plays a crucial role in MM-osteocyte interactions by enhancing the osteoclastogenic potential of osteocytes through increased RANKL production. Further, we discovered that CCL3 stimulates the active release of HMGB1 by osteocytes, which may act as a propagating pro-osteoclastogenic signal in neighboring osteocytes. Both clinical and preclinical data, supported by pharmacologic and genetic studies in human and mouse models, reinforce these findings. Our results expand our understanding of the multifunctional role of CCL3 in MM and uncover new molecular interactions between osteocytes and MM cells, emphasizing the importance of these interactions in MM progression.

References

1. Rajkumar SV. Multiple myeloma: 2020 update on diagnosis, risk-stratification and management. Am J Hematol. 2020;95(5):548-567.
2. Diaz-delCastillo M, Chantry AD, Lawson MA, Heegaard AM. Multiple myeloma-A painful disease of the bone marrow. Semin Cell Dev Biol. 2021;112:49-58.
3. Horsboel TA, Nielsen CV, Andersen NT, Nielsen B, de Thurah A. Risk of disability pension for patients diagnosed with haematological malignancies: a register-based cohort study. Acta Oncol. 2014;53(6):724-734.
4. Roodman GD. Pathogenesis of myeloma bone disease. Leukemia. 2009;23(3):435-441.
5. Delgado-Calle J, Anderson J, Cregor MD, et al. Bidirectional Notch Signaling and Osteocyte-Derived Factors in the Bone Marrow Microenvironment Promote Tumor Cell Proliferation and Bone Destruction in Multiple Myeloma. Cancer Res. 2016;76(5):1089-1100.
6. Lai FP, Cole-Sinclair M, Cheng WJ, et al. Myeloma cells can directly contribute to the pool of RANKL in bone bypassing the classic stromal and osteoblast pathway of osteoclast stimulation. Br J Haematol. 2004;126(2):192-201.
7. Xiong J, Onal M, Jilka RL, Weinstein RS, Manolagas SC, O'Brien CA. Matrix-embedded cells control osteoclast formation. Nat Med. 2011;17(10):1235-1241.
8. Nakashima T, Hayashi M, Fukunaga T, et al. Evidence for osteocyte regulation of bone homeostasis through RANKL expression. Nat Med. 2011;17(10):1231-1234.
9. Delgado-Calle J. Osteocytes and their messengers as targets for the treatment of multiple myeloma. Clin Rev Bone Miner Metab. 2017;15(1):49-56.

10. Toscani D, Bolzoni M, Ferretti M, Palumbo C, Giuliani N. Role of Osteocytes in Myeloma Bone Disease: Anti-sclerostin Antibody as New Therapeutic Strategy. Front Immunol. 2018;24:9:2467.
11. Sabol HM, Ashby C, Adhikari M, et al. A NOTCH3-CXCL12-driven myeloma-tumor niche signaling axis promotes chemoresistance in multiple myeloma. Haematologica. 2024;109(8):2606-2618.
12. Sabol HM, Amorim T, Ashby C, et al. Notch3 signaling between myeloma cells and osteocytes in the tumor niche promotes tumor growth and bone destruction. Neoplasia. 2022;28:100785.
13. Sabol HM, Ferrari AJ, Adhikari M, et al. Targeting Notch Inhibitors to the Myeloma Bone Marrow Niche Decreases Tumor Growth and Bone Destruction without Gut Toxicity. Cancer Res. 2021;81(19):5102-5114.
14. Fu Q, Bustamante-Gomez NC, Reyes-Pardo H, et al. Reduced OPG expression by osteocytes may contribute to rebound resorption after denosumab discontinuation. JCI Insight. 2023;8(18):e167790.
15. Simonet WS, Lacey DL, Dunstan CR, et al. Osteoprotegerin: a novel secreted protein involved in the regulation of bone density. Cell. 1997;89(2):309-319.
16. Choi SJ, Cruz JC, Craig F, et al. Macrophage inflammatory protein 1-alpha is a potential osteoclast stimulatory factor in multiple myeloma. Blood. 2000;96(2):671-675.
17. Han JH, Choi SJ, Kurihara N, Koide M, Oba Y, Roodman GD. Macrophage inflammatory protein-1alpha is an osteoclastogenic factor in myeloma that is independent of receptor activator of nuclear factor kappaB ligand. Blood. 2001;97(11):3349-3353.

18. Vallet S, Pozzi S, Patel K, et al. A novel role for CCL3 (MIP-1α) in myeloma-induced bone disease via osteocalcin downregulation and inhibition of osteoblast function. Leukemia. 2011;25(7):1174-1181.

19. Roussou M, Tasidou A, Dimopoulos MA, et al. Increased expression of macrophage inflammatory protein-1alpha on trephine biopsies correlates with extensive bone disease, increased angiogenesis and advanced stage in newly diagnosed patients with multiple myeloma. Leukemia. 2009;23(11):2177-2181.

20. Terpos E, Politou M, Viniou N, Rahemtulla A. Significance of macrophage inflammatory protein-1 alpha (MIP-1alpha) in multiple myeloma. Leuk Lymphoma. 2005;46(12):1699-1707.

21. Hashimoto T, Abe M, Oshima T, et al. Ability of myeloma cells to secrete macrophage inflammatory protein (MIP)-1alpha and MIP-1beta correlates with lytic bone lesions in patients with multiple myeloma. Br J Haematol. 2004;125(1):38-41.

22. Terpos E, Politou M, Szydlo R, Goldman JM, Apperley JF, Rahemtulla A. Serum levels of macrophage inflammatory protein-1 alpha (MIP-1alpha) correlate with the extent of bone disease and survival in patients with multiple myeloma. Br J Haematol. 2003;123(1):106-109.

23. Uneda S, Hata H, Matsuno F, et al. Macrophage inflammatory protein-1 alpha is produced by human multiple myeloma (MM) cells and its expression correlates with bone lesions in patients with MM. Br J Haematol. 2003;120(1):53-55.

24. Bidwell JP, Yang J, Robling AG. Is HMGB1 an osteocyte alarmin? J Cell Biochem. 2008;103(6):1671-1680.

25. Davis HM, Valdez S, Gomez L, et al. High mobility group box 1 protein regulates osteoclastogenesis through direct actions on osteocytes and osteoclasts in vitro. J Cell Biochem. 2019;120(10):16741-16749.

26. Greipp PR, San Miguel J, Durie BG, et al. International staging system for multiple myeloma. J Clin Oncol. 2005;23(15):3412-3420.

27. Roodman GD. Pathogenesis of myeloma bone disease. J Cell Biochem. 2010;109(2):283-291.

28. Tsubaki M, Kato C, Isono A, et al. Macrophage inflammatory protein-1α induces osteoclast formation by activation of the MEK/ERK/c-Fos pathway and inhibition of the p38MAPK/IRF-3/IFN-β pathway. J Cell Biochem. 2010;111(6):1661-1672.

29. Oba Y, Lee JW, Ehrlich LA, et al. MIP-1alpha utilizes both CCR1 and CCR5 to induce osteoclast formation and increase adhesion of myeloma cells to marrow stromal cells. Exp Hematol. 2005;33(3):272-278.

30. Choi SJ, Oba Y, Gazitt Y, et al. Antisense inhibition of macrophage inflammatory protein 1-alpha blocks bone destruction in a model of myeloma bone disease. J Clin Invest. 2001;108(12):1833-1841.

31. Tsubaki M, Kato C, Manno M, et al. Macrophage inflammatory protein-1alpha (MIP-1alpha) enhances a receptor activator of nuclear factor kappaB ligand (RANKL) expression in mouse bone marrow stromal cells and osteoblasts through MAPK and PI3K/Akt pathways. Mol Cell Biochem. 2007;304(1-2):53-60.

32. Han JH, Choi SJ, Kurihara N, Koide M, Oba Y, Roodman GD. Macrophage inflammatory protein-1alpha is an osteoclastogenic factor in myeloma that is independent of receptor activator of nuclear factor kappaB ligand. Blood. 2001;97(11):3349-3353.

33. Toscani D, Palumbo C, Dalla PB, et al. The Proteasome Inhibitor Bortezomib Maintains Osteocyte Viability in Multiple Myeloma Patients by Reducing Both Apoptosis and Autophagy: A New Function for Proteasome Inhibitors. J Bone Miner Res. 2016;31(4):815-827.

34. Giuliani N, Ferretti M, Bolzoni M, et al. Increased osteocyte death in multiple myeloma patients: role in myeloma-induced osteoclast formation. Leukemia. 2012;26(6):1391-1401.

35. Davis HM, Pacheco-Costa R, Atkinson EG, et al. Disruption of the Cx43/miR21 pathway leads to osteocyte apoptosis and increased osteoclastogenesis with aging. Aging Cell. 2017;16(3):551-563.

36. Geduk A, Oztas B, Eryılmaz BH, et al. Effects of AGEs, sRAGE and HMGB1 on Clinical Outcomes in Multiple Myeloma. Indian J Hematol Blood Transfus. 2023;39(2):220-227.

37. Casciaro M, Vincelli D, Ferraro M, et al. The role of High-mobility group box-1 and Psoriasin in multiple myeloma: Analysis of a population affected by monoclonal gammopathies and review of the literature. Pathol Res Pract. 2023;247:154562.

38. Chen R, Kang R, Tang D. The mechanism of HMGB1 secretion and release. Exp Mol Med. 2022;54(2):91-102.

39. Liu H, He J, Bagheri-Yarmand R, et al. Osteocyte CIITA aggravates osteolytic bone lesions in myeloma. Nat Commun. 2022;13(1):3684.

40. Oyajobi BO, Franchin G, Williams PJ, et al. Dual effects of macrophage inflammatory protein-1alpha on osteolysis and tumor burden in the murine 5TGM1 model of myeloma bone disease. Blood. 2003;102(1):311-319.

41. Abe M, Hiura K, Ozaki S, Kido S, Matsumoto T. Vicious cycle between myeloma cell binding to bone marrow stromal cells via VLA-4-VCAM-1 adhesion and macrophage

inflammatory protein-1alpha and MIP-1beta production. J Bone Miner Metab. 2009;27(1):16-23.

42. Reyes C, Hitz M, Prieto-Alhambra D, Abrahamsen B. Risks and Benefits of Bisphosphonate Therapies. J Cell Biochem. 2016; 117(1):20-28.
43. Aspenberg P, Schilcher J. Atypical femoral fractures, bisphosphonates, and mechanical stress. Curr Osteoporos Rep. 2014;12(2):189-193.
44. Raje N, Terpos E, Willenbacher W, et al. Denosumab versus zoledronic acid in bone disease treatment of newly diagnosed multiple myeloma: an international, double-blind, double-dummy, randomised, controlled, phase 3 study. Lancet Oncol. 2018;19(3):370-381.
45. Drejer LA, El-Masri BM, Ejersted C, et al. Trabecular bone deterioration in a postmenopausal female suffering multiple spontaneous vertebral fractures due to a delayed denosumab injection - A post-treatment re-initiation bone biopsy-based case study. Bone Rep. 2023;19:101703.
46. Kim AS, Girgis CM, McDonald MM. Osteoclast Recycling and the Rebound Phenomenon Following Denosumab Discontinuation. Curr Osteoporos Rep. 2022;20(6):505-515.
47. Zeissig MN, Hewett DR, Mrozik KM, et al. Expression of the chemokine receptor CCR1 decreases sensitivity to bortezomib in multiple myeloma cell lines. Leuk Res. 2024;139:107469.
48. Du J, Lin Z, Fu XH, Gu XR, Lu G, Hou J. Research progress of the chemokine/chemokine receptor axes in the oncobiology of multiple myeloma (MM). Cell Commun Signal. 2024;22(1):177.

49. Liu L, Yu Z, Cheng H, et al. Multiple myeloma hinders erythropoiesis and causes anaemia owing to high levels of CCL3 in the bone marrow microenvironment. Sci Rep. 2020;10(1):20508.

50. Zeissig MN, Hewett DR, Panagopoulos V, et al. Expression of the chemokine receptor CCR1 promotes the dissemination of multiple myeloma plasma cells in vivo. Haematologica. 2021;106(12):3176-3187.

51. Tsubaki M, Takeda T, Tomonari Y, et al. The MIP-1α autocrine loop contributes to decreased sensitivity to anticancer drugs. J Cell Physiol. 2018;233(5):4258-4271.

52. Dairaghi DJ, Oyajobi BO, Gupta A, et al. CCR1 blockade reduces tumor burden and osteolysis in vivo in a mouse model of myeloma bone disease. Blood. 2012;120(7):1449-1457.

Figure legends

Figure 1. Multiple myeloma cells upregulate *Rankl* mRNA expression in mature and early osteocytes. *Rankl* expression in bones infiltrated by human JJN3 (A) or murine 5TGM1 (B) multiple myeloma (MM) cells. N=7-10 mice/group. *p<0.05 vs. mice injected with saline (Veh) by Student's *t*-test. Boxes show the data interquartile range, the middle line in the box represents the median, and whiskers the 95% confidence interval of the mean (A, B). *Rankl* expression in murine Ocy-454 (mature), MLO-Y4 (mature), and MLO-A5 (early) osteocyte (Ot)-like cell lines treated with 48 hours (h)-conditioned media (CM) from human JJN3 cells (C) or murine 5TGM1 (D) MM cells. N=4-6/group. *p<0.05 vs. cell treated with Veh by Student's *t*-test for each time point. Data are shown as mean ± SD. Representative experiments out of two are shown (C, D).

Figure 2. CCL3 expression is increased in bones infiltrated with multiple myeloma cells. Kaplan-Meier plot of the (A) overall survival (OS) and (B) progression-free survival (PFS) of newly diagnosed multiple myeloma (NDMM) patients with high (Hi) vs. low (Lo) *CCL3* expression. N=708 patients. Data were analyzed using a Log-rank (Mantel-Cox) test. Human (Hs; left) and murine (Mm; right) *CCL3* mRNA expression in bones infiltrated by human JJN3 (C) or murine 5TGM1 (D) multiple myeloma (MM) cells. N=7-10 mice/group. *p<0.05 vs. mice injected with saline (Veh) by Student's *t*-test. Boxes show the data interquartile range, the middle line in the box represents the median, and whiskers the 95% confidence interval of the mean (C, D). (E) *Ccr1, 3, and 5* expression in murine Ocy-454 (mature), MLO-Y4 (mature), and MLO-A5 (early) osteocyte (Ot)-like cell lines. N=3-6/group. *p<0.05 vs. Ccr1 expression by One-way ANOVA, followed by a Tukey post hoc test. Data are shown as mean ± SD. Representative experiments out of two are shown (E).

Figure 3. Multiple myeloma-derived CCL3 increases RANKL production in osteocytes. (A) *Rankl* expression in murine Ocy-454 (mature), MLO-Y4 (mature), and MLO-A5 (early) osteocyte (Ot)-like cell lines treated with recombinant CCL3 (1μg/mL). N=4-6/group. *p<0.05 vs. cell treated with vehicle (Veh) by Student's *t*-test for each time point. (B) *Rankl* expression in murine bones cultured *ex vivo* and treated with recombinant CCL3 (1μg/mL) for 2 days. N=4/group. *p<0.05 vs. bones treated with Veh by Student's *t*-test for each time point. (C) RANKL protein levels in murine Ocy-454 Ot-like cell lines treated with recombinant CCL3 (1μg/mL) or 48h-conditioned media (CM) from control (Ctl) or *CCL3* knocked down ($CCL3^{KD}$) JJN3 multiple myeloma (MM) cells for 2 days. N=4/group. *p<0.05 vs. cell treated with Veh by Two-way ANOVA, followed by a Tukey post hoc test. *Rankl* expression in murine Ocy-454, MLO-Y4, and MLO-A5 Ot-like cell lines treated with 48h-CM from human JJN3 (D) or murine 5TGM1 (E) MM cells in the presence/absence of a neutralizing antibody against CCL3 (CCL3-Ab; 50 ng/mL) for 1 day. N=4-6/group. *p<0.05 as indicated by the lines by One-way ANOVA, followed by a Tukey post hoc test. Data are shown as mean ± SD. Representative experiments out of two are shown.

Figure 4. Genetic inhibition of CCL3 in multiple myeloma cells decreases tumor growth and attenuates bone destruction. (A) *CCL3* expression in human JJN3 multiple myeloma (MM) cells. N=3/group. *p<0.05 vs. cell treated with vehicle (Veh) by Student's *t*-test for each week (wk). (B) Tumor progression in mice injected with Veh, control (Ctl), or *CCL3* knocked down ($CCL3^{KD}$) JJN3 cells. N=10 mice/group. *p<0.05 vs. mice injected with Veh by One-way ANOVA, followed by a Tukey post hoc test. Data are shown as mean (square, circle, and triangle symbols) ± SD (dashed lines) (A, B). (C) Representative micro-CT 3D bone reconstructions of tibias, (D) longitudinal tibiae cancellous bone volume/tissue volume (BV/TV)

quantification, and (E) percent change in cancellous BV/TV (before/after cell injection) in mice injected with Veh or Ctl or *CCL3*^{KD} MM cells. N=10 mice/group. *p<0.05 as indicated by lines by One-way ANOVA, followed by a Tukey post hoc test. Boxes show the data interquartile range, the middle line in the box represents the median, and whiskers the 95% confidence interval of the mean (D, E).

Figure 5. Genetic inhibition of CCL3 in multiple myeloma cells decreases RANKL upregulation in osteocytes. (A) Representative images and prevalence of *Rankl*$^{+}$ primary osteocytes in bones from mice injected with vehicle (Veh), control (Ctl), or *CCL3* knocked down (*CCL3*^{KD}) JJN3 multiple myeloma (MM) cells after 4 weeks. N=10 mice/group. *p<0.05 as indicated by lines by One-way ANOVA, followed by a Tukey post hoc test. Black arrows indicate *Rankl*$^{+}$ osteocytes. Blue dashed lines indicate the bone surface. (B) Levels of the tumor biomarker Kappa light chain in the conditioned media (CM) and *RANKL*, *OPG*, and *CCL3* mRNA expression in e*x vivo* human bone-MM cell organ cultures established with Veh or Ctl or *CCL3*^{KD} MM JJN3 cells and femoral head bone fragments from healthy human donors after 4 days. N=6 bones/group. *p<0.05 as indicated by lines by One-way ANOVA, followed by a Tukey post hoc test. (C) *RANKL*, *OPG*, and *CCL3* mRNA expression in e*x vivo* organ cultures established with femoral head bone fragments from two healthy human donors treated with Veh or 48h-CM from Ctl or *CCL3*^{KD} MM JJN3 cells during 3 days. N=8 bones/group. *p<0.05 as indicated by lines by One-way ANOVA, followed by a Tukey post hoc test. Data are shown as mean ± SD (A, B, C).

Figure 6. Multiple myeloma-derived CCL3 stimulates HMGB1 secretion in osteocytes. *Hmgb1* expression in bones infiltrated by human JJN3 (A) or murine 5TGM1 (B) multiple myeloma (MM) cells. N=6 mice/group. *p<0.05 vs. mice injected with saline (Veh) by Student's

t-test. Boxes show the data interquartile range, the middle line in the box represents the median, and whiskers the 95% confidence interval of the mean (A, B). HMGB1 protein levels in murine Ocy-454 Ot-like cells treated with (C) 48h-conditioned media (CM) from control (Ctl) or *CCL3* knocked down ($CCL3^{KD}$) JJN3 cells for 3 days or with 48h-CM from JJN3 in the presence/absence of a neutralizing antibody against CCL3 (50 ng/mL) for 2 days. N=5/group. *p<0.05 as indicated by lines by One- (C) or Two-way (D) ANOVA, followed by a Tukey post hoc test. Data are shown as mean ± SD (C, D). Representative experiments out of two are shown (C, D).

Figure 7. Autocrine HMGB1 signaling facilitates the stimulation of osteocyte RANKL production triggered by multiple myeloma-derived CCL3. *Rankl* expression in murine Ocy-454 (mature), MLO-Y4 (mature), and MLO-A5 (early) osteocyte (Ot)-like cell lines treated with 48h-conditioned media (CM) from human JJN3 cells (A) or murine 5TGM1 (B) multiple myeloma (MM) cells in the presence/absence of a neutralizing antibody against HMGB1 (HMGB1-Ab; 10 μg/mL) for 1 day. N=4-6/group. *p<0.05 as indicated by lines by Two-Way ANOVA, ANOVA, followed by a Tukey post hoc test. (C) *Rankl* expression in Ocy-454 and MLO-A5 Ot-like cell lines with/without genetic silencing of *Hmgb1* and treated with 48h-CM from human JJN3 cells for 1 day. N=4/group. *p<0.05 as indicated by lines by Two-Way ANOVA, followed by a Tukey post hoc test. (D) HMGB1 protein levels in murine Ocy-454 Ot-like cells with/without genetic silencing of *Hmgb1* and treated with 48h-CM from human JJN3 cells for 2 days. N=4/group. *p<0.05 as indicated by lines by Two-Way ANOVA, followed by a Tukey post hoc test. (E) *Rankl* expression in murine bones cultured *ex vivo* and treated with recombinant CCL3 (1μg/mL) with/without HMGB1-Ab (10μg/mL) for 2 days. *p<0.05 as

indicated by lines by Two-Way ANOVA, followed by a Tukey post hoc test. Data are shown as mean ± SD. Representative experiments out of two are shown (A-E).

Figure 8. Multiple myeloma patients exhibit increased *RANKL* and HMGB1 expression in osteocytes. Representative images of histological sections of bone biopsies and blow out of osteocytes from a representative healthy subject (A and C) and a multiple myeloma (MM) patient (B and D) stained for nuclei (blue), *RANKL* mRNA expression (orange), and HMGB1 protein expression (pink). White dashed lines define the mineralized bone. (C) AI-assisted quantitative analysis of the prevalence of $RANKL^+$, $HMGB1^+$, and double $RANKL^+$-$HMGB1^+$ osteocytes (n=5-6/group). *$p<0.05$ vs. healthy subjects (control) by Student's *t*-test. Data are shown as mean ± SEM; each dot represents an independent sample.

Figure 1

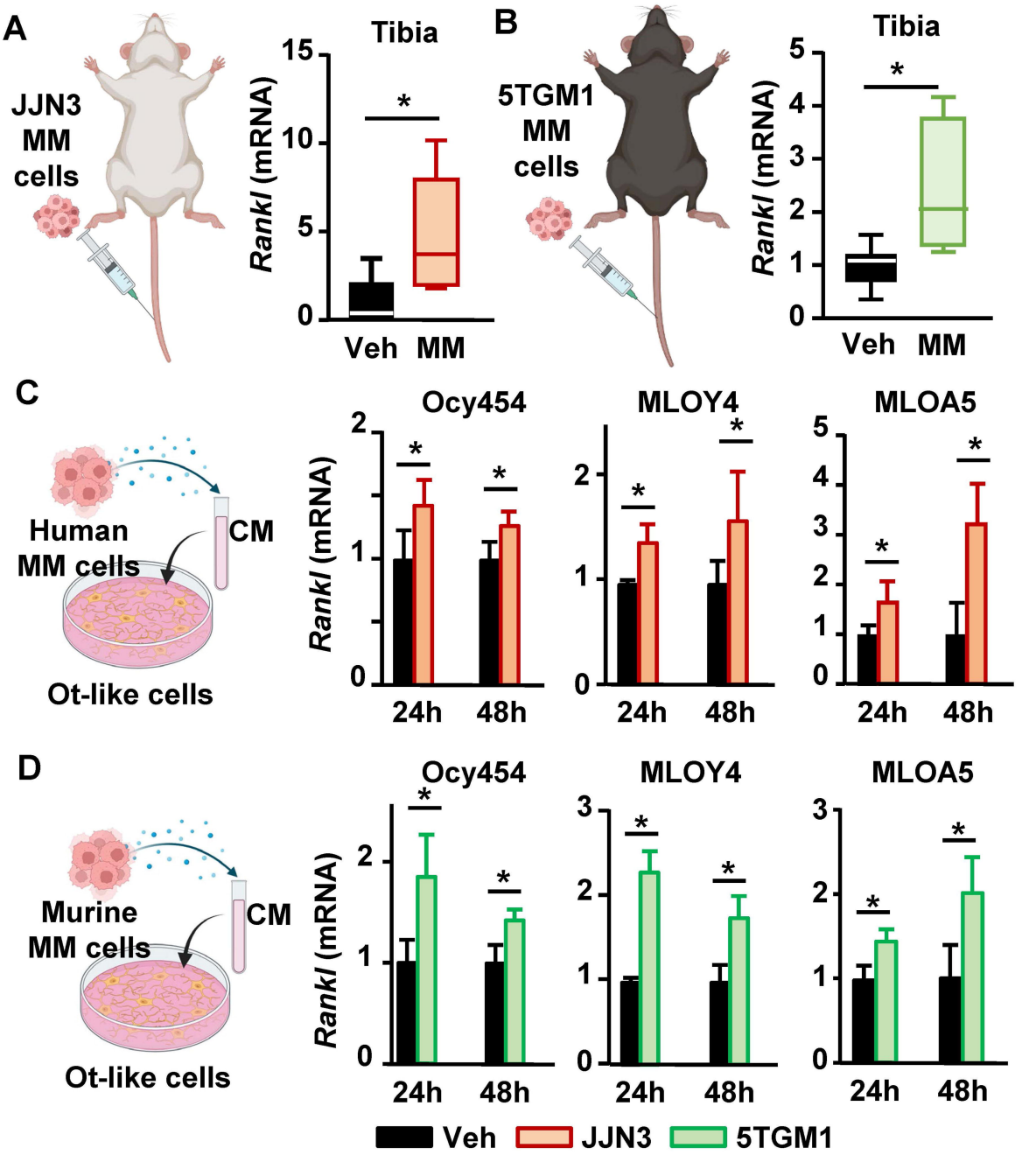
A
JJN3
MM
cells
Tibia
Rankl (mRNA)
15
10
5
0
*
Veh
MM
B
5TGM1
MM
cells
Tibia
Rankl (mRNA)
5
4
3
2
1
0
*
Veh
MM
C
Human
MM cells
CM
Ot-like cells
Ocy454
MLOY4
MLOA5
Rankl (mRNA)
2
1
0
5
4
3
*
24h
48h
D
Murine
MM cells
CM
Ot-like cells
Ocy454
MLOY4
MLOA5
Rankl (mRNA)
3
2
1
0
*
24h
48h
Veh
JJN3
5TGM1

Figure 2

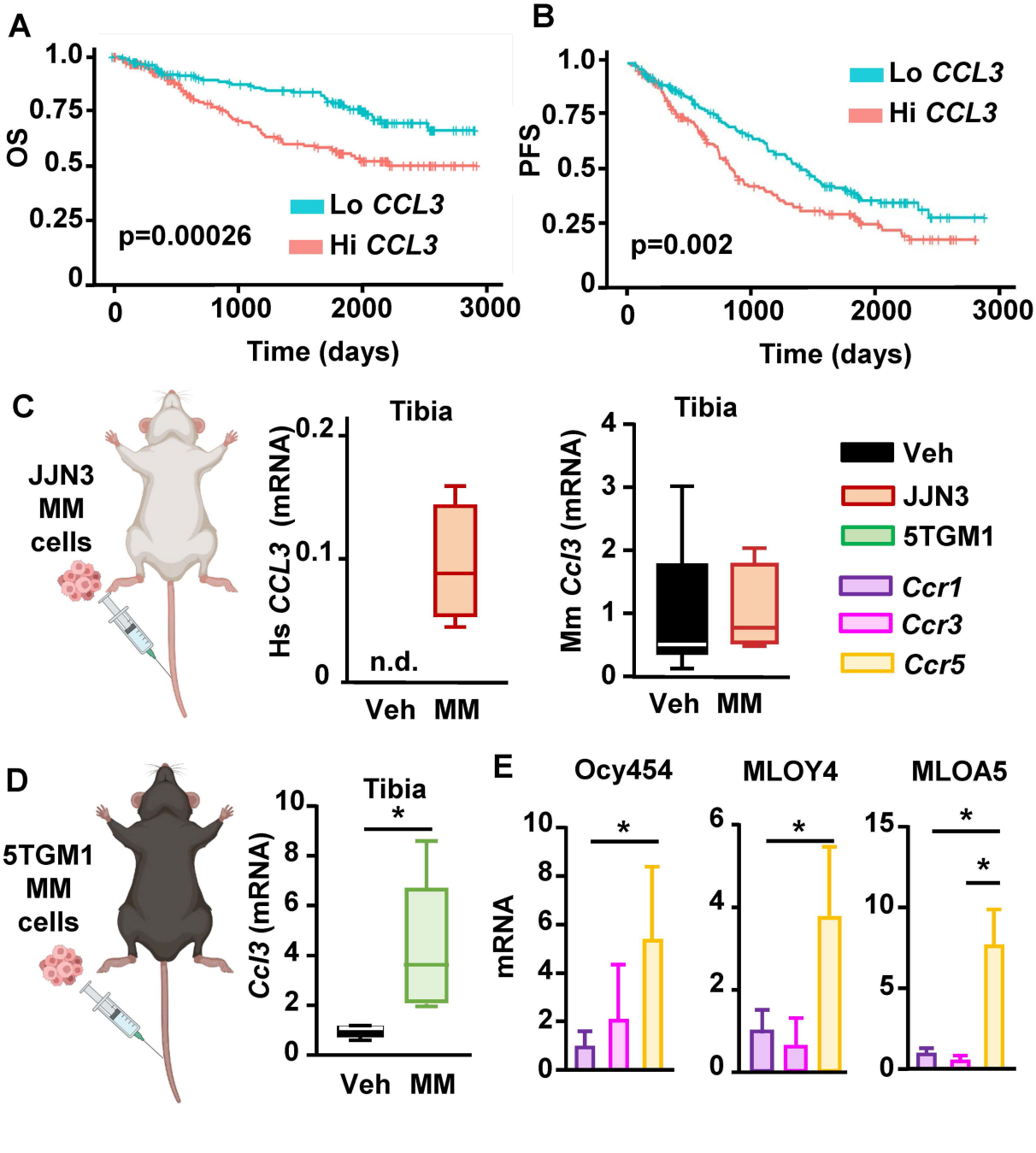
A
OS
1.0
0.75
0.5
0.25
0
p=0.00026
Lo CCL3
Hi CCL3
0
1000
2000
3000
Time (days)
B
PFS
1.0
0.75
0.5
0.25
0
p=0.002
Lo CCL3
Hi CCL3
0
1000
2000
3000
Time (days)
C
JJN3
MM
cells
Tibia
Hs CCL3 (mRNA)
0.2
0.1
0
n.d.
Veh
MM
Tibia
Mm Ccl3 (mRNA)
4
3
2
1
0
Veh
MM
Veh
JJN3
5TGM1
Ccr1
Ccr3
Ccr5
D
5TGM1
MM
cells
Tibia
Ccl3 (mRNA)
10
8
6
4
2
0
*
Veh
MM
E
Ocy454
MLOY4
MLOA5
mRNA
10
8
6
4
2
0
*
6
4
2
0
*
15
10
5
0
*
*

Figure 3

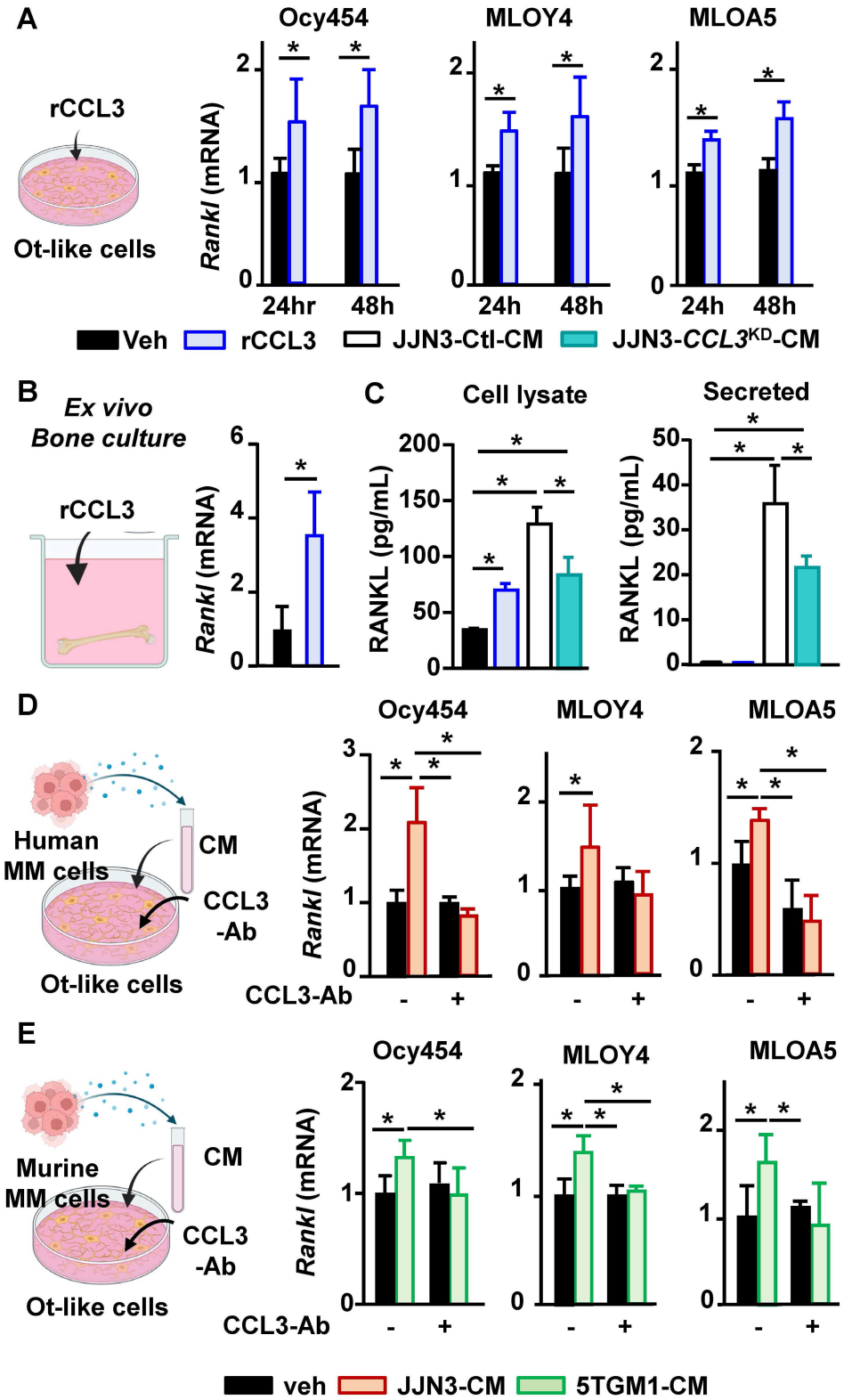
A
rCCL3
Ot-like cells
Ocy454
MLOY4
MLOA5
Rankl (mRNA)
24hr
48h
Veh
rCCL3
JJN3-Ctl-CM
JJN3-CCL3KD-CM
B
Ex vivo
Bone culture
rCCL3
Rankl (mRNA)
C
Cell lysate
Secreted
RANKL (pg/mL)
D
Human
MM cells
CM
CCL3
-Ab
Ot-like cells
Ocy454
MLOY4
MLOA5
Rankl (mRNA)
CCL3-Ab
E
Murine
MM cells
CM
CCL3
-Ab
Ot-like cells
Ocy454
MLOY4
MLOA5
Rankl (mRNA)
CCL3-Ab
veh
JJN3-CM
5TGM1-CM

Figure 4

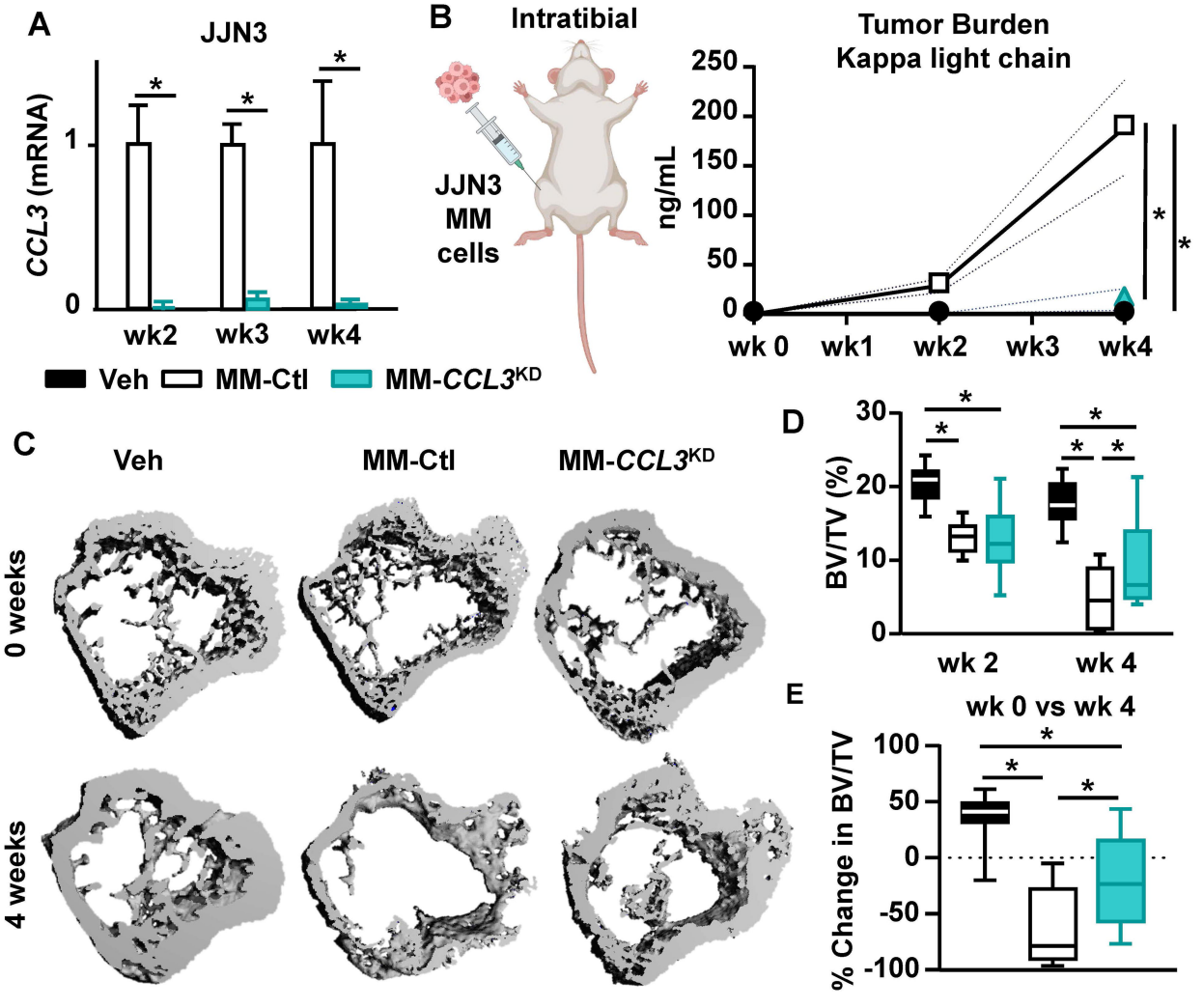
A
JJN3
CCL3 (mRNA)
1
0
wk2
wk3
wk4
Veh
MM-Ctl
MM-CCL3KD
B
Intratibial
JJN3
MM
cells
Tumor Burden
Kappa light chain
250
200
150
100
50
0
ng/mL
wk 0
wk1
wk2
wk3
wk4
C
Veh
MM-Ctl
MM-CCL3KD
0 weeks
4 weeks
D
30
20
10
0
BV/TV (%)
wk 2
wk 4
E
wk 0 vs wk 4
100
50
0
-50
-100
% Change in BV/TV

Figure 5

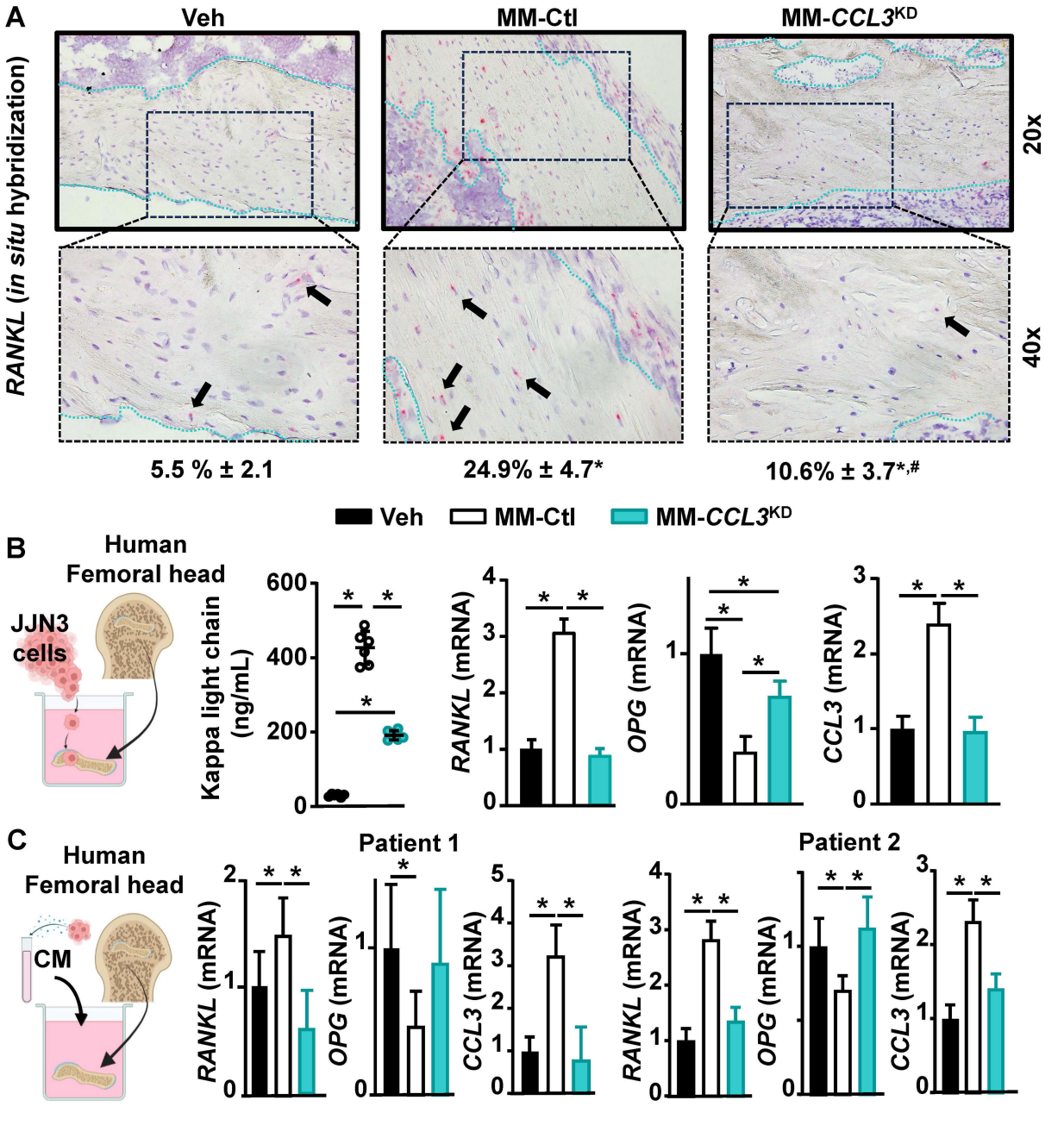
A
Veh
MM-Ctl
MM-CCL3KD
RANKL (in situ hybridization)
20x
40x
5.5 % ± 2.1
24.9% ± 4.7*
10.6% ± 3.7*,#
Veh
MM-Ctl
MM-CCL3KD
B
Human
Femoral head
JJN3
cells
Kappa light chain
(ng/mL)
600
400
200
0
RANKL (mRNA)
OPG (mRNA)
CCL3 (mRNA)
C
Human
Femoral head
CM
Patient 1
Patient 2
RANKL (mRNA)
OPG (mRNA)
CCL3 (mRNA)

Figure 6

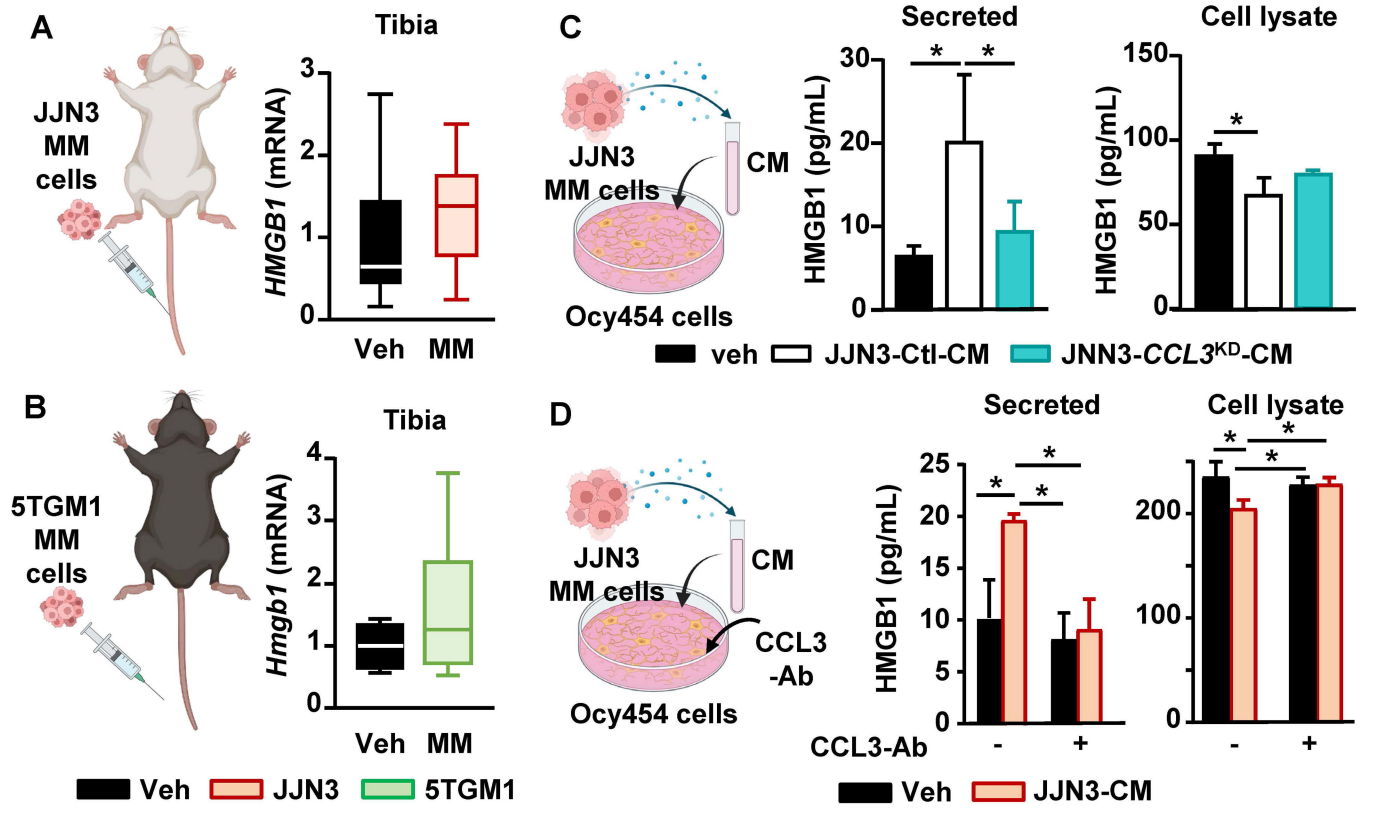
A
JJN3
MM
cells
Tibia
HMGB1 (mRNA)
3
2
1
0
Veh
MM
B
5TGM1
MM
cells
Tibia
Hmgb1 (mRNA)
4
3
2
1
0
Veh
MM
Veh
JJN3
5TGM1
C
JJN3
MM cells
CM
Ocy454 cells
Secreted
HMGB1 (pg/mL)
30
20
10
0
*
*
Cell lysate
HMGB1 (pg/mL)
150
100
50
0
*
veh
JJN3-Ctl-CM
JNN3-CCL3KD-CM
D
JJN3
MM cells
CM
CCL3
-Ab
Ocy454 cells
Secreted
HMGB1 (pg/mL)
25
20
15
10
5
0
*
*
*
Cell lysate
200
100
0
*
*
*
CCL3-Ab
-
+
-
+
Veh
JJN3-CM

Figure 7

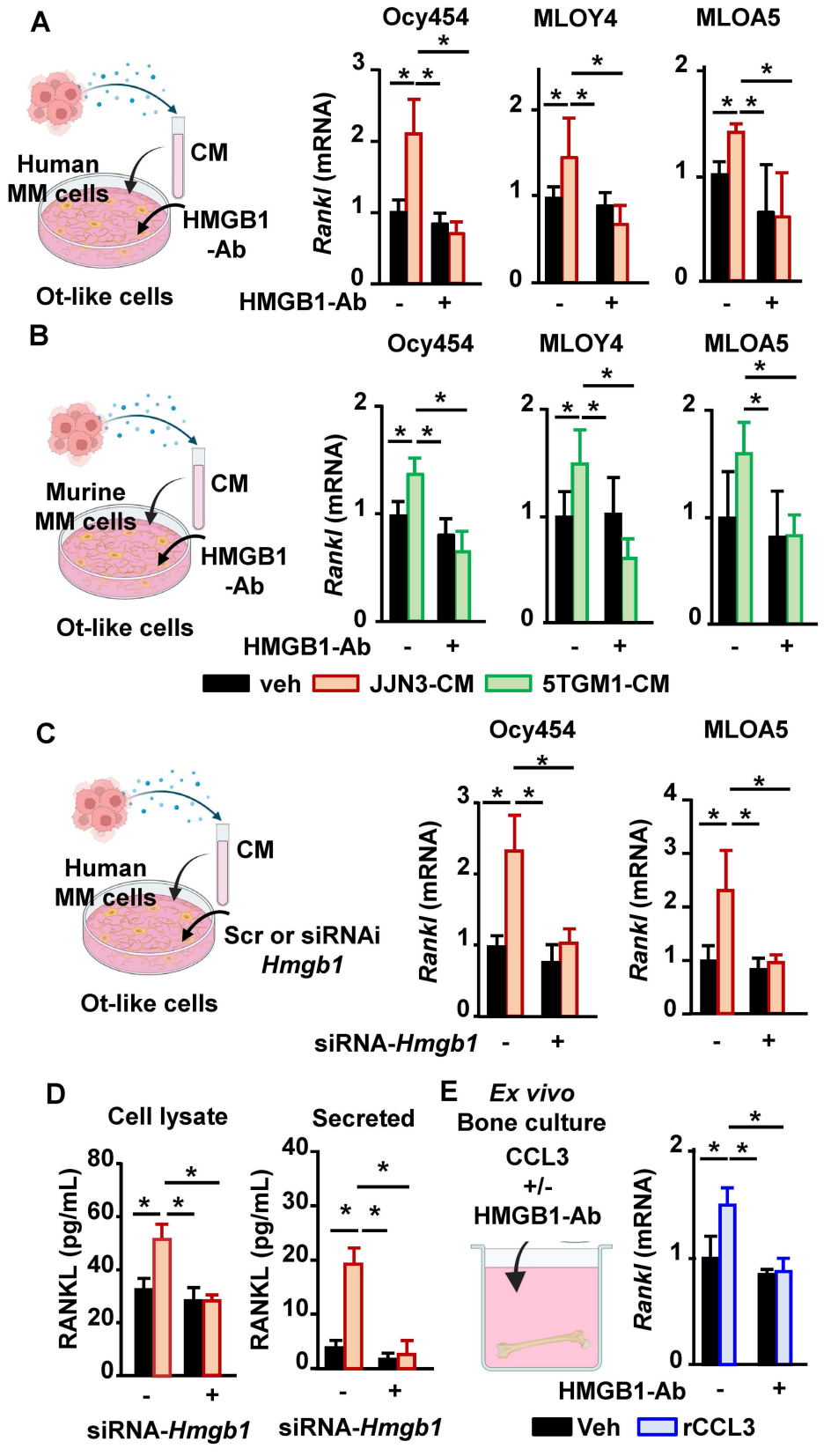
A
Ocy454
MLOY4
MLOA5
Human MM cells
CM
HMGB1 -Ab
Ot-like cells
Rankl (mRNA)
HMGB1-Ab - +
B
Murine MM cells
veh
JJN3-CM
5TGM1-CM
C
siRNA-Hmgb1
Scr or siRNAi Hmgb1
D
Cell lysate
Secreted
RANKL (pg/mL)
E
Ex vivo
Bone culture
CCL3
+/-
HMGB1-Ab
Veh
rCCL3

Figure 8

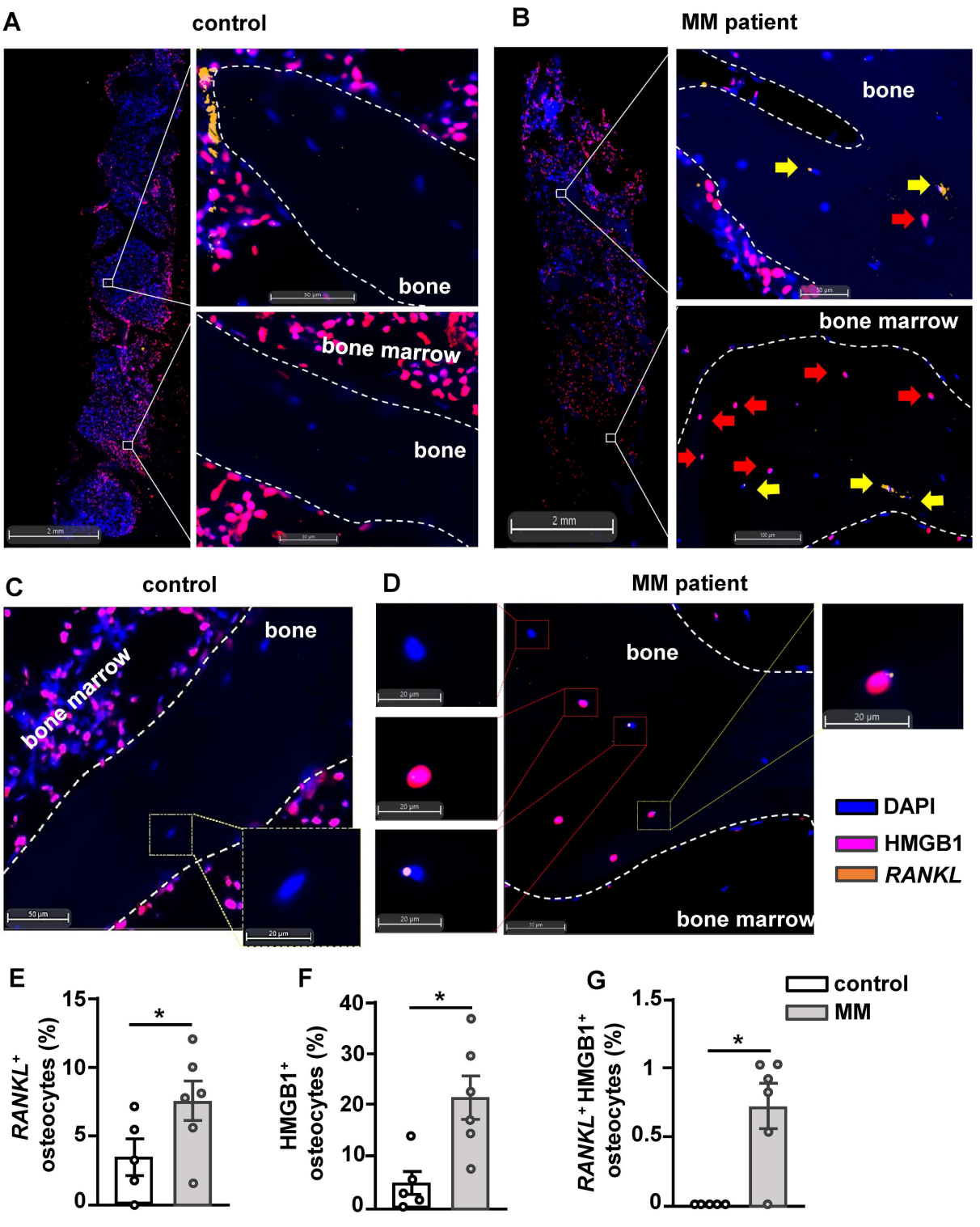
A
control
bone
bone marrow
bone
2 mm
B
MM patient
bone
bone marrow
2 mm
C
control
bone
bone marrow
50 µm
20 µm
D
MM patient
bone
bone marrow
20 µm
DAPI
HMGB1
RANKL
E
RANKL+ osteocytes (%)
15
10
5
0
*
F
HMGB1+ osteocytes (%)
40
30
20
10
0
*
G
control
MM
RANKL+HMGB1+ osteocytes (%)
1.5
1
0.5
0
*

Supplementary Methods.

Reagents. RPMI 1640 media, Minimum Essential Media (MEM) α, Opti-MEM, fetal bovine serum, bovine calf serum, Normocin, antibiotics (penicillin/streptomycin), and TriZol were purchased from Invitrogen Life Technologies (Grand Island, NY, USA). Trypan Blue and the anti-HMGB1 neutralizing antibody (Cat. #H9537, RRID:AB 260090) were purchased from Millipore Sigma (Burlington, MA, USA). Recombinant CCL3 (Cat. #270-LD-010/CF) and the anti- CCL3 neutralizing antibody (Cat. #MAB270-500, RRID:AB_2070775) were purchased from R&D Systems (Minneapolis, MN, USA). The *CCL3* sgRNA CRISPR/spCas9 lentiviral particles were purchased from Applied Biological Materials Inc. (Richmond, BC, CA, Cat. #sc-417845) and the *Hmgb1* mouse siRNA Oligo Duplex (Locus ID: 15289; Cat. #SR426038) were purchased from Origene Technology Inc. (Richmond, BC, Canada). Puromycin (Cat#58-58-2) was purchased from InvivoGen (San Diego, CA, USA).

Human samples methods and histological analysis. Bone biopsies of 3-mm diameter were fixed in 4% paraformaldehyde and decalcified in 0.5M EDTA prior to paraffin embedding. Formalin-fixed paraffin-embedded (FFPE) tissues were sectioned into 3.5-µm thickness and deparaffinized in a xylene-ethanol gradient. Slides were incubated in TE buffer overnight at 60°C, blocked with 5% casein/Tris-buffered saline (TBS), and incubated for 2 hours with a monoclonal mouse antibody against HMGB1 (Thermo Fisher Scientific, Cat # MA5-17278; RRID: AB_2538744). The signal was amplified with horse radish peroxidase-conjugated anti-mouse IgG polymers (BrightVision, Duiven, Holland) for 30 minutes at room temperature and revealed with opal 620 dye (Akoya Biosciences, Marlborough, MA, USA). Thereafter, sections were incubated in Custom Reagent (Advanced Cell Diagnostics, Hayward, CA, USA) for 20 min at 40°C and hybridized overnight at 40°C with a 20-basepair probe targeting *RANKL* mRNA within the target region

between base pairs 366 and 1507 (NM_003701.3; Advanced Cell Diagnostics, Hayward, CA, USA). The day after, signal amplification was performed following the manufacturer´s recommendations and visualized with opal 570 dye (Akoya Biosciences, Marlborough, MA, USA). Sections were Hoechst counterstained, mounted in Prolong Gold (Fisher Scientific, Roskilde, Denmark), and scanned in a VS200 Olympus Slidescanner (Tokyo, Japan). Scans were obtained at 40X with 40 ms exposure in the DAPI channel and 100 ms exposure in the Cy3 (565 nm) and Texas Red Kromigon (615 nm) channels); visualization settings were similar across all images during quantification, and differentially adjusted to capture representative images. Negative controls were performed by omission of the primary antibody/hybridization probe. Analyses were performed by a researcher blinded to study groups using artificial intelligence-assisted histology in the IF-FISH v2.1.5 HALO module (v3.6.4134, Indica Labs). Briefly, trabecular bone was manually delimited, and cellular *RANKL* and HMGB1 expression were automatically quantified; $RANKL^{+}$ osteocytes presenting >4 copies/cell were excluded from analyses.

Genetic inhibition in MM cells and osteocyte-like cells.

To generate stable *CCL3* knockdown cells ($CCL3^{KD}$), JJN3 MM cells were transduced with *CCL3* sgRNA CRISPR/Cas9 lentiviral particles (MOI=10) and selected with 3.0ug/mL Puromycin over 4 weeks. To transiently knockdown *CCL3* in MM cells or *Hmgb1* in Ocy454s, cells were incubated with 50μM of *CCL3* human or *Hmgb1* mouse siRNA Oligo Duplex in alpha-MEM complete media with15% Opti-MEM and 0.4% lipofectamine for 48hrs.

***Ex vivo* Bone Organ Cultures.** Murine *ex vivo* bone organ cultures were established with tibiae and/or femurs from C57BL/KaLwRijHsd (murine MM cells) or NSG (human MM cells) mice, as described before.[1-4] Murine bones were treated with 1ug/mL or recombinant CCL3 in the

presence/absence of 10µg/mL of anti-HMGB1 for 24 hours. Human *ex vivo* bone organ cultures were established using human cancellous bone fragments similar in size obtained from the femoral head of patients with no pathologies or medications that could affect bone mass or architecture discarded after hip arthroplasty.[5] For these *ex vivo* cultures, $2x10^5$ Ctl or *CCL3*^{KD} JJN3 MM cells were plated on human bones or bones were treated with 48h-CM from Ctl or *CCL3*^{KD} JJN3 MM cells for 3 days. Treatments were refreshed daily.

Gene mRNA expression. Total RNA was isolated from MM cells, osteocyte-like cells, and bone tissues using Trizol and converted to cDNA (Invitrogen Life Technologies), following the manufacturer's directions. RNA was converted to cDNA, and gene expression was quantified by qPCR using Taqman assays from Applied Biosystems (Foster City, CA, USA). Values were normalized by *Gapdh* or *ChoB* expression. Gene expression levels were calculated using the comparative threshold (CT) method.

Enzyme-linked immunosorbent assays (ELISA). ELISAs for RANKL (R&D Systems, Cat. #MTR00) and HMGB1 (Fischer Scientific, Cat. #EEL102) were performed according to the manufacturer's instructions. Conditioned media was concentrated using Amicon® ultra-centrifugal Filter (10kDa; Cat. #UFC20124) according to the manufacturer's instructions. Cell protein lysates were obtained using Pierce™ RIPA buffer (Fisher Scientific, Cat. #89900) with a protease inhibitor cocktail (Fisher Scientific, Cat. #4906837001 and phosphatase inhibitor (Millipore Sigma, Cat. #4906837001), then quantified using the Pierce™ BCA assay (MilliporeSigma, Cat. #23228/23224). Cell lysates were loaded onto the ELISAs using 100µg of protein/well.

Western Blots. Protein was loaded in 10% SDS-PAGE gels. Proteins were transferred to PVDF membranes. Immunoblots were performed using anti-HMGB1(Cat. #3935s, Cell Signaling Technology Inc., Danvers, MA, USA) and anti-albumin (Cat. #NBP2-26510, Novus Biologicals

Inc., Centennial, CO, USA) followed by goat anti-rabbit secondary antibodies, conjugated to horseradish peroxidase (1:2000). Western blots were developed using the chemiluminescence detection assay.

References

1. Sabol HM, Ashby C, Adhikari M, et al. A NOTCH3-CXCL12-driven myeloma-tumor niche signaling axis promotes chemoresistance in multiple myeloma. Haematologica. 2024;
2. Sabol HM, Amorim T, Ashby C, et al. Notch3 signaling between myeloma cells and osteocytes in the tumor niche promotes tumor growth and bone destruction. Neoplasia. 2022;28(100785.
3. Delgado-Calle J, Anderson J, Cregor MD, et al. Bidirectional Notch Signaling and Osteocyte-Derived Factors in the Bone Marrow Microenvironment Promote Tumor Cell Proliferation and Bone Destruction in Multiple Myeloma. Cancer Res. 2016;76(5):1089-1100.
4. Bellido T, Delgado-Calle J. Ex Vivo Organ Cultures as Models to Study Bone Biology. JBMR Plus. 2020;4(3):
5. Adhikari M, Kaur J, Sabol HM, et al. Single-cell Transcriptome Analysis Identifies Senescent Osteocytes as Contributors to Bone Destruction in Breast Cancer Metastasis. PREPRINT (Version 1) available at Research Square [https://doiorg/1021203/rs3rs-4047486/v1]. 2024;

Suppl. Fig 1

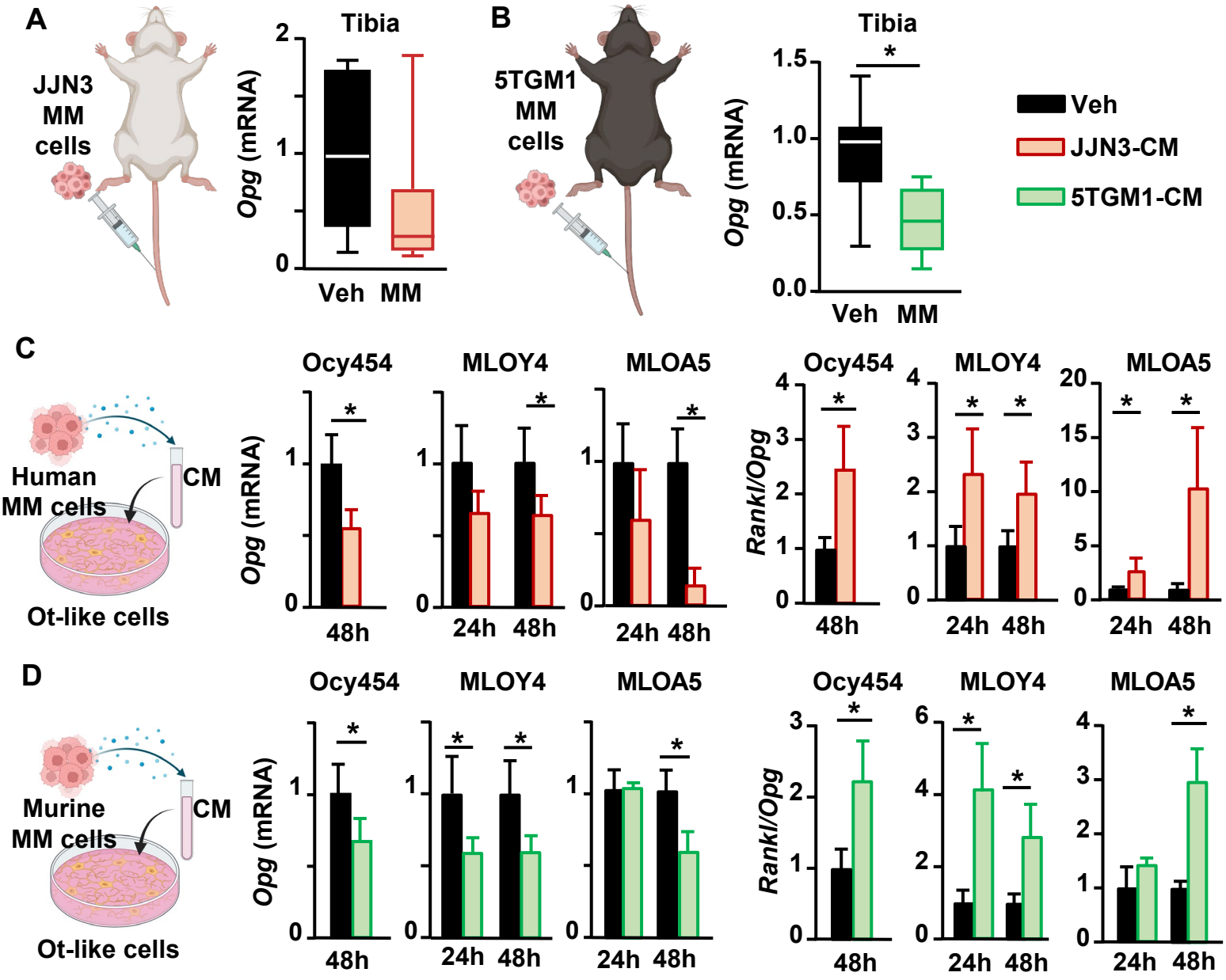

Suppl. Figure 1. Multiple myeloma cells increase the *Rankl/Opg ratio* in osteocytes. *Opg* expression and *Rankl/Opg* ratio in murine Ocy-454 (mature), MLO-Y4 (mature), and MLO-A5 (early) osteocyte (Ot)-like cell lines treated with 48h-conditioned media (CM) from human JJN3 cells (A) or murine 5TGM1 (B) multiple myeloma (MM) cells. N=4/group. *p<0.05 vs. cell treated with Veh by Student's *t*-test for each time point. Data are shown as mean ± SD. Representative experiments out of two are shown.

Suppl. Fig 2

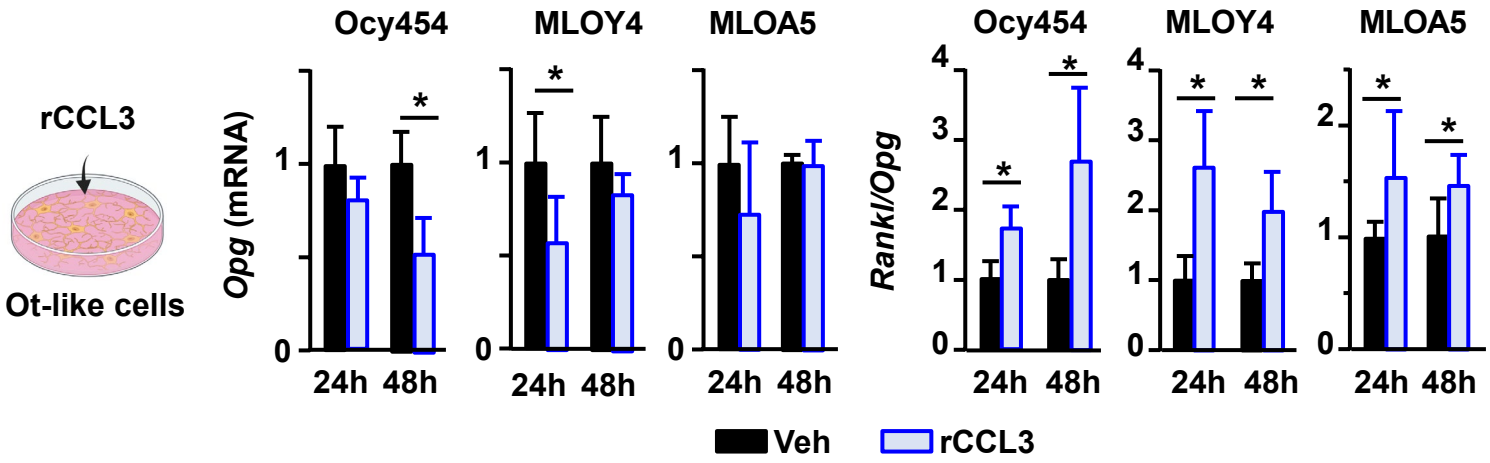

Suppl. Figure 2. Recombinant CCL3 increases the Rankl/Opg ratio in osteocytes. *Opg* expression and *Rankl/Opg* ratio in murine Ocy-454 (mature), MLO-Y4 (mature), and MLO-A5 (early) osteocyte (Ot)-like cell lines treated with recombinant CCL3 (1µg/mL). N=4-6/group. *p<0.05 vs. cell treated with Veh by Student's *t*-test for each time point. Data are shown as mean ± SD. Representative experiments out of two are shown.

Suppl. Fig 3

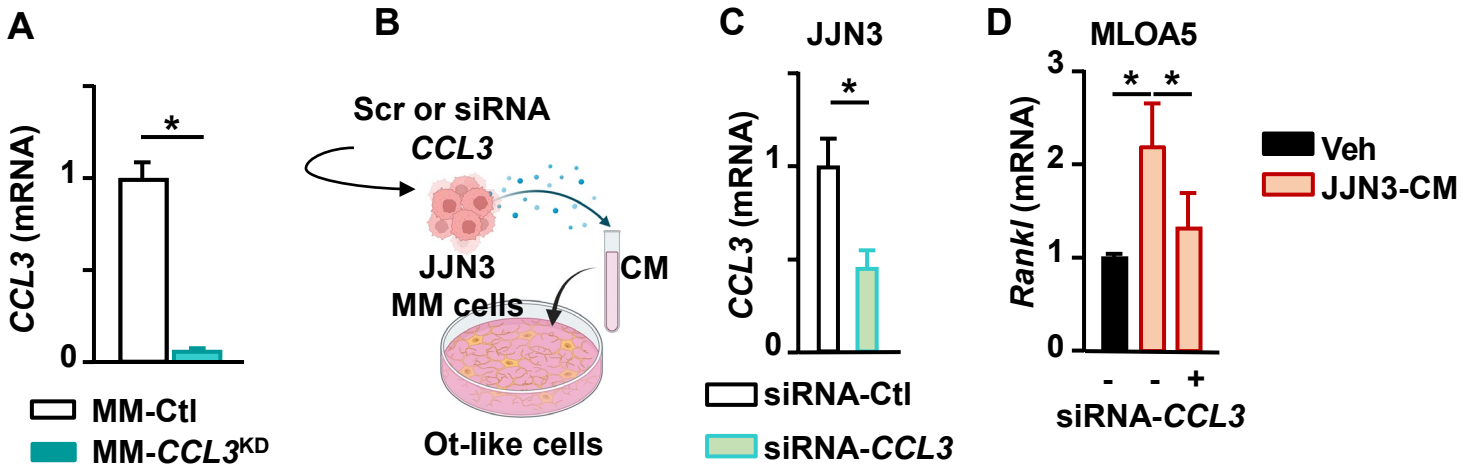

Suppl. Figure 3. siRNA-mediated inhibition of *CCL3* in multiple myeloma cells prevents *Rankl* upregulation in osteocytes by multiple myeloma cells. (A) CCL3 expression in control (Ctl) and CCL3 knockdown human JJN3 multiple myeloma (MM) cells. N=4/group. *p<0.05 vs. cells treated with Veh by Student's t-test. (B) Experimental design. (C) *CCL3* expression in human JJN3 MM cells treated with control (Ctl)- or *CCL3*-siRNAs for 48h. N=4-6/group. *p<0.05 vs. cell treated with Veh by Student's *t*-test. (D) *Rankl* expression in murine MLO-A5 osteocyte-like cells treated with Ctl- or *CCL3*-siRNA and cultured with/without 48h-CM from human JJN3 for 1 day. N=4-6/group. *p<0.05 as indicated by the lines by One-way ANOVA, followed by a Tukey post hoc test. Data are shown as mean ± SD. Representative experiments out of two are shown.

Suppl. Fig 4

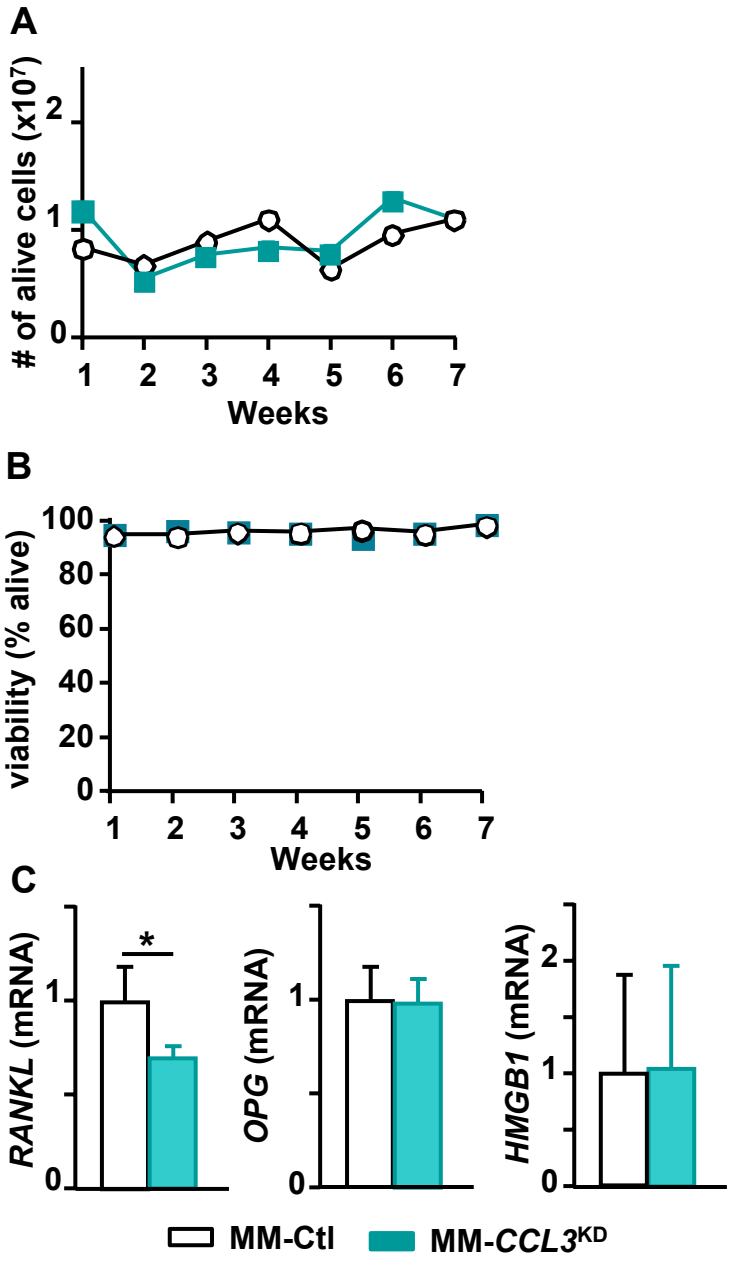

Suppl. Figure 4. Cellular and molecular characterization of human JJN3 multiple myeloma cells with *CCL3* knockdown. Cell number (A), cell viability (B), and (C) *RANKL*, *OPG*, and *HMGB1* expression in control (Ctl) and *CCL3* knockdown human JJN3 multiple myeloma (MM) cells. N=4/group. *p<0.05 vs. cells treated with Veh by Student's *t*-test. Data are shown as mean ± SD. Representative experiments out of two are shown.

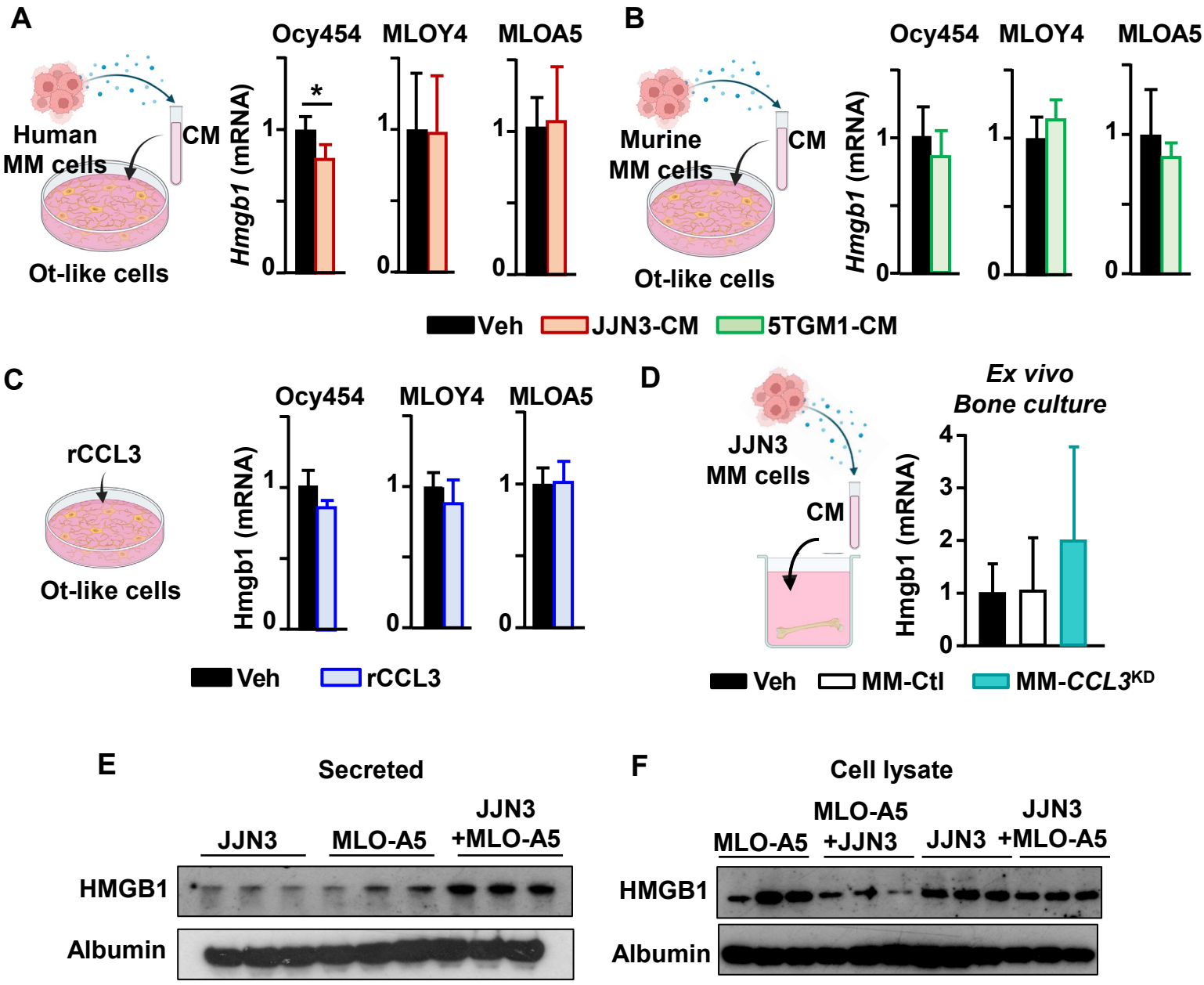

Suppl. Figure 5. Multiple myeloma cells stimulate HMGB1 release by osteocytes. *Hmgb1* expression in murine Ocy-454 (mature), MLO-Y4 (mature), and MLO-A5 (early) osteocyte (Ot)-like cell lines treated with (A) 48h-conditioned media (CM) from human JJN3 multiple myeloma (MM) cells, (B) CM from murine 5TGM1-MM cells (B), or (C) recombinant (r) CCL3 (1μg/mL) for 1 day. N=4-6/group. *$p<0.05$ vs. cell treated with Veh by Student's *t*-test for each time point. (D) *Hmgb1* expression in murine bones cultured *ex vivo* and treated CM from control (Ctl) or *CCL3* knocked down (*CCL3*^{KD}) JJN3 cells for 2 days. N=4-6/group. (E) Secreted HMGB1 detected in the conditioned media of human JJN3 MM cells or MLO-A5 osteocyte-like cell cultures alone or co-cultured for 48h. (F) HMGB1 detected in cell lysates from human JJN3 MM cells or murine MLO-A5 osteocyte-like cells cultured alone or co-cultured for 48h. Data are shown as mean ± SD. Representative experiments out of two are shown (A, B, C, D).

Suppl. Fig 6

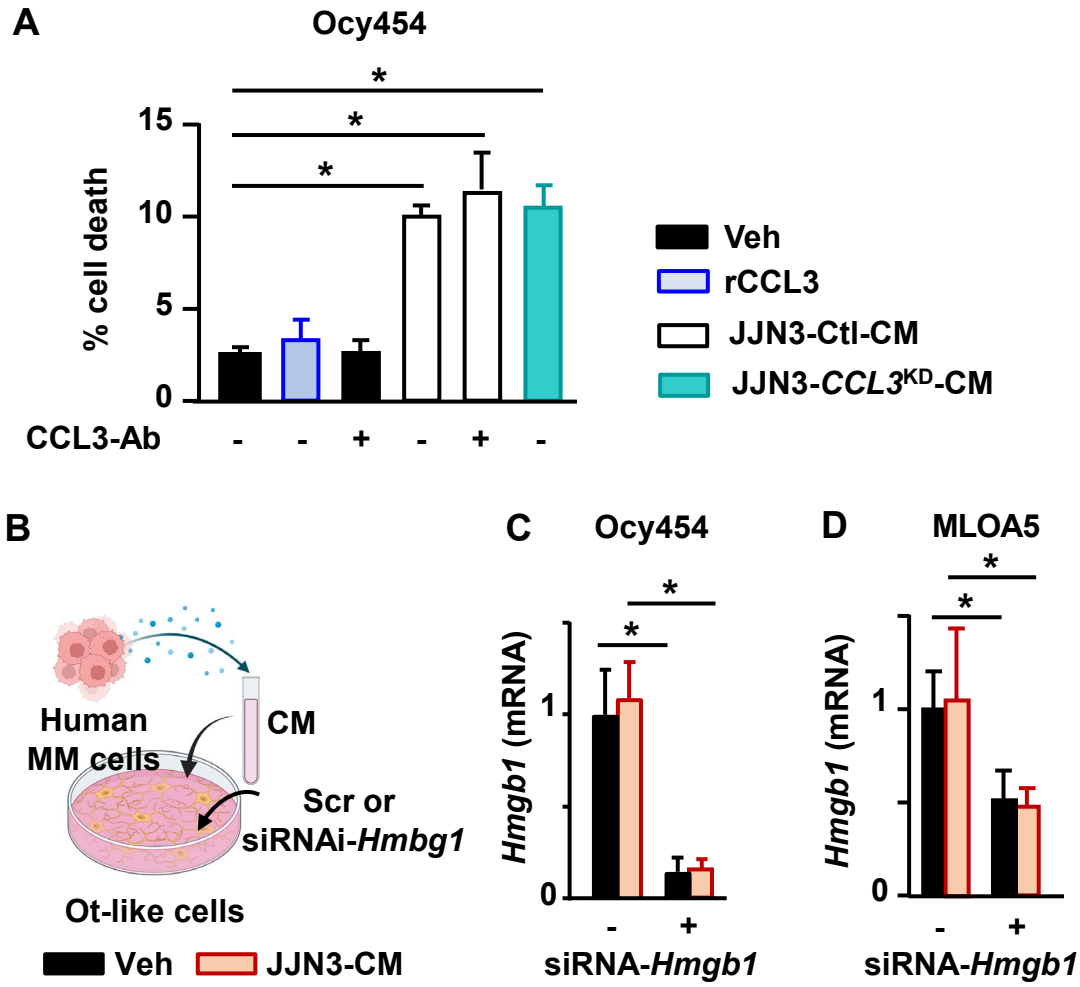

Suppl. Figure 6. Osteocytic HMGB1 release mediates the *Rankl* upregulation in osteocytes induced by MM cells. (A) Cell death in Ocy-454 osteocyte (ot)-like cells treated with recombinant CCL3, anti-CCL3 antibody (CCL3-Ab), or 48h-conditioned media (CM) from control (Ctl)- or *CCL3* knockdown human JJN3 MM cells for 1 day. N=4/group. *p<0.05 as indicated by the lines by One-way ANOVA, followed by a Tukey post hoc test. (B) Experimental design. *Hmgb1* expression in murine Ocy-454 (C) or MLO-A5 (D) Ot-like cell lines treated with/without control (Ctl)- or *Hmgb1*-siRNA and cultured in the presence/absence of 48h-CM from human JJN3 MM cells for 1 days. N=4/group. *p<0.05 as indicated by the lines by Two-way ANOVA, followed by a Tukey post hoc test. Data are shown as mean ± SD. Representative experiments out of two are shown.